

Calibration and Validation for the Surface Biology and Geology (SBG) Mission Concept: Challenges of a Multi-Sensor System for Imaging Spectroscopy and Thermal Imagery

Kevin R. Turpie¹, Kimberly Casey², Christopher J. Crawford³, Liane S. Guild⁴, Hugh Kieffer⁵, Guoqing (Gary) Lin⁶, Raymond Kokaly⁷, Alok Shrestha⁴, Cody Anderson³, Shankar N. Chandra⁸, Robert Green⁹, Simon Hook⁹, Constantine Lukashin¹⁰, Kurt Thome⁷, Robert E. Wolfe⁶

¹ University of Maryland, Baltimore County.

² US Geological Survey, Reston Virginia.

³ US Geological Survey, Earth Resources Observation and Science Center

⁴ NASA Ames Research Center.

⁵ Celestial Reasonings, Genoa Nevada.

⁶ NASA Goddard Space Flight Center.

⁷ US Geological Survey, Boulder Colorado.

⁸ KBR Incorporated.

⁹ California Institute of Technology.

¹⁰ NASA Langley Research Center.

Corresponding author: K.R. Turpie (kturpie@umbc.edu)

Key Points:

- Provides an overview of calibration ideas developed for the SBG mission concept.
- Looks at approaches to inter-calibration of multiple Earth orbiting sensors.
- Surveys what calibration and validation resources are currently available or may be available to the SBG mission later in this decade.

Abstract

The primary objective of the NASA Surface Biology and Geology (SBG) mission is to measure biological, physical, chemical, and mineralogical features of the Earth's surface, realizing the conceptual component of the envisioned NASA Earth System Observatory (ESO). SBG is planned to launch as a two-platform mission in the late 2020s, the first of the ESO satellites. Targeted science and applications objectives based on observations of the Earth's surface biology and geology helped to define the mission architecture and instrument capabilities for the SBG mission concept. These objectives further drove the need for enabling change detection and trending of surface biological and geological features. These needs implied fundamental

calibration goals to achieve the necessary science data quality characteristics. To meet those goals, calibration and validation pre-launch and on-orbit methods formed a basis of the calibration and validation concept, including the combined use of on-board references, vicarious techniques, and routine lunar imaging. International collaboration with space agencies in other countries, an important feature of the recommended SBG mission architecture, uncovered and emphasized the need for inter-calibration techniques that underscored the importance of collaborative instrument characterization data sharing and the use of common calibration references that are International System of Units (SI) traceable in pre-launch and post-launch on orbit calibration mission phases. International collaboration through the use of terrestrial and aquatic networks on six continents for vicarious calibration and validation activities will produce unprecedented data quality.

1 Introduction

The SBG Designated Observable (DO) science and application objectives, as outlined in the 2017 National Academies of Science, Engineering and Medicine Committee on Earth Science and Application from Space (ESAS) Decadal Survey report (NASEM 2018), were used to conceptualize the SBG mission architecture. These objectives included global observation, change detection and trending of terrestrial and aquatic surface ecosystems, hydrology, geology and their effect on weather and climate. Measurements must be able to detect seasonal and long-term changes for addressing dynamics of the Earth System and Essential Climate Variables (ECV) to advance the investigations of climatic change and impacts. To address the global scope of the science, SBG must provide global coverage of land, island, and coastal and inland waters. These objectives and observations were described in the Science and Applications Traceability Matrix (SATM) described by Stavros et al. (2022) and summarized in Table 1.

These needs drove choices of mission architecture and instrument characterization and performance and further established fundamental calibration and validation goals needed to achieve the implied science data quality characteristics. First, to acquire said Earth observations globally with sufficient spatial, spectral and temporal resolutions and ranges, NASA will use two separate free-flying platforms, each in low-Earth, polar, sun-synchronous orbits. These orbits must provide consistent Sun-sensor geometry for consistency in retrievals and for calibration and validation, and provide for consistent global coverage. One satellite would be in a descending morning orbit similar to Landsat and support a imaging spectrometer covering wavelengths from ~ 0.4 to $2.5 \mu\text{m}$ (i.e., visible-to-shortwave infrared or VSWIR) and another satellite in ascending afternoon orbit carrying a multi-band, thermal infrared (TIR) imager. The target launch date of the two-platform mission is early 2028, making these the first of the Earth System Observatory (ESO) satellites planned by NASA to fly.

In addition, in order to improve temporal sampling, the SBG mission architecture was extended to include potential cooperation with agencies of other nations. Two independent, polar-orbiting VSWIR imaging spectrometers from ESA's Copernicus Hyperspectral Imaging Mission for the Environment (CHIME) would potentially complement the SBG VSWIR imaging spectrometer. In addition, two polar-orbiting thermal imagers from ESA's Copernicus Land Surface Temperature Monitoring (LSTM) and the future polar-orbiting thermal imager of the Thermal infraRed Imaging Satellite for High-resolution Natural resource Assessment (TRISHNA) planned by CNES and ISRO, would likewise complement the SBG thermal imager. The desired

harmonization of observations from these multiple platforms implied the need for inter-calibration techniques, which likewise underscored the further need for collaborative sharing of instrument characterization data, the use of common reference data, and the implementation of data harmonization.

The SBG mission architecture and its intended science and application objectives naturally led to the decisions for support of pre-launch and on-orbit calibration elements, including the combined use of an on-board reference and the Moon and employing of vicarious calibration using terrestrial and aquatic targets. Calibration validation strategies are critical to meeting the science and applications objectives outlined in Stavos et al (2022). These strategies determine whether measurement quality will be sufficient in terms of radiometric accuracy, data product quality and temporal stability.

The SBG project initially chartered the Calibration and Validation Working Group (CVWG) to scope, establish, and recommend calibration and validation strategies for SBG observations with input from the global imaging spectroscopy community. The CVWG is led by Kevin Turpie (UMBC / NASA GSFC) and Ray Kokaly (USGS) and includes, but is not limited to the co-authors of this paper, and extends to dozens of domestic and international organizations. Initially, the CVWG identified a set of high-level calibration and validation schemes that would constitute plans for pre-launch and post-launch calibration of SBG VSWIR and TIR instruments and validation of calibrated data products derived from remote measurements. This included scoping pre-launch instrument characterization activities, defining potential objectives for vicarious and on-orbit calibration, and describing validation strategies for mission data products. The CVWG also considered the need to identify calibration reference sites and measurements to satisfy post-launch calibration and validation objectives. The CVWG also evaluated basic needs for data product validation from the calibrated measurements above the top-of-atmosphere (TOA) based on a broad concept of what data products might be provided. This involved the identification of external *in situ* measurement resources and organizations through which appropriate vicarious calibration and validation activities could be conducted. An initial inventory of these potential resources was created to help scope the SBG validation concept and determine what may be available for vicarious calibration. Further work is expected to continue through the mission development life cycle, especially closer to launch to reduce the risk that such resources might not be available during flight and allow for further development of data product quality requirements. This paper provides an overview of the SBG mission calibration concept with consideration for inter-calibration needs among collaborating Earth observation missions on data product harmonization agreements and provides numerous recommendations by the SBG CVWG.

Further development of SBG calibration and validation strategies will come with the formulation of the SBG mission. Fortunately, with close to 40 years of experience with airborne imaging spectrometers (such as AIS, Vane et al., 1984; AVIRIS-Classic, Green et al, 1998; AVIRIS-NG, Chapman et al., 2019; and HyMap, Cocks et al, 1998) there is broadening experience with such instruments and data with many recent imaging spectrometer missions operating from space, including CHRIS on PROBA-1 (Barnsely et al., 2004), the Chinese Tiangong-1 (Li et al., 2016), the Italian PRISMA mission (Pignatti et al., 2013), Japan's HISUI (Iwasaki et al., 2011), the German DESIS sensor (Krutz et al., 2019), as well as new missions such as the German EnMAP (Alonso et al., 2019) launched April 2022, NASA's EMIT launched July 2022 (Green et al.,

2022), the Israeli/Italian SHALOM mission concept (Feingersh and Ben Dor, 2015), and ESA's FLEX mission (Coppo et al., 2017). Further, synergies with other NASA hyperspectral satellite missions, namely Plankton, Aerosol, Cloud, ocean Ecosystem (PACE, planned launch 2024) and Geostationary Littoral Imaging and Monitoring Radiometer (GLIMR, planned launch 2026) will enable calibration and validation concept testing and implementation prior to SBG launch.

2 Recommendations Towards Cross-Mission Commonality

2.1 Common Metrological Language and Terms for Spaceborne Remote Sensing Techniques

The intent of this section is to propose some common terminology and use those terms to provide further background behind the calibration and validation concepts that are described in this paper. The SBG CVWG recommended that SBG and collaborating missions establish a common metrological and radiometric language to clearly define metrological terms in a common language and, where possible, derived from international standards (e.g., Ferrero, 2009; BIPM, 2008; Schaepman-Strub et al., 2006; Nicodemus et al., 1977) specific to imaging spectroscopy and thermal imaging. This metrological lexicon should include, but not be limited to terms such as 'calibration,' 'validation,' 'uncertainty,' 'accuracy,' 'precision,' and 'reflectance.' Of particular interest for common terms and definitions for the imaging spectroscopy community is the IEEE P4001 working group effort, which is ongoing, for setting hyperspectral standards for VSWIR imaging spectrometers (Durell, 2019; <https://standards.ieee.org/project/4001.html>).

For the purposes of this paper, the SBG CVWG defines and distinguishes 'calibration' and 'validation' as unique mission components as outlined by the Committee on Earth Observation Satellites Working Group on Calibration and Validation (CEOS WGCV). The process of 'calibration' is quantitatively defining a system's response to known and controlled signal inputs (CEOS <https://ceos.org/ourwork/workinggroups/wgcv/>).

In the context of this paper, we take calibration simply as the act of making a one-to-one association of a physical measurement scale to an instrument response. For the SBG mission, three types of physical measurement scales are of import:

1. **Radiometric** scale (including thermal scale), which places a scale in physical units on instrument response in the form of a digital readout. The scale is in units of radiance or reflectance in the VSWIR measurements or brightness temperature for TIR measurements. For reflectance, *a priori* information regarding solar irradiance is required.
2. **Spectral** scale, which assigns wavelength positions to spectral channels and defines the bandpasses of the spectral channels (their responses as a function of wavelength, which is commonly modeled with gaussian or similar mathematical function for imaging spectrometers and is defined as the spectral response function for broadband sensors).
3. **Geometric** scale, a multi-dimensional metric, which ultimately facilitates geolocation, i.e., placing spectra on a spatial grid and determines sensor-sun geometry.

A key focus of this paper is radiometric calibration because that will present the greatest challenge to intercalibration. However, aspects regarding establishing geolocation and a

wavelength scale are discussed, especially given that they are important to radiometric intercalibration and accuracy and ultimately to data harmonization.

Calibration is 'absolute' if it can associate a measurement scale that is traceable to national or international standards with an instrument system response. A calibration is 'relative' if it adjusts a previously mapped scale relative to some other presumably more accurate scale. Relative calibration usually involves characterizing differences, either between two instruments or with the same instrument with changing conditions or with time. To adjustments based on comparisons over time, Müller (2014) gave the term re-calibration. In this latter case of relative calibration, removal of drift in instrument response over time is made by trending or monitoring instrument behavior. For convenience, the SBG CVWG refers to this as a 'time-dependent calibration'.

Vicarious calibration is any radiometric calibration method that uses stable materials on the Earth's surface as a reference. Earth's surface may be well-characterized pseudo-invariant, sites that are actively instrumented *in situ* (e.g., RadCalNet; Bouet et al., 2019), or sites that are episodically measured during field campaigns, for example, during a commissioning phase or later evaluation period (Storch et al., 2014). The modifier 'vicarious' is used because a spaceborne instrument is being indirectly calibrated using instruments on the ground, i.e., transferring radiometric scales from instruments on Earth to a spaceborne instrument using the Earth's surface as an intermediate reference. All vicarious calibration for Earth observing satellites must contend with the Earth's atmosphere to some degree, especially targets that have relatively low reflectance (e.g., deep, clear water).

The terms inter-calibration and cross-calibration appear in the literature as interchangeable, but we will only use the term inter-calibration to establish absolute calibration scales on two or more instruments producing measurements that agree within expected uncertainty. This usually involves use of a common, well known reference by all instruments being inter-calibrated. This could include either the transfer of a scale from another more accurately calibrated instrument using near identical observations (i.e., close in time and geometry) or a well-characterized source.

The measurements of two instruments can be compared for inter-consistency. The general use of statistical comparisons of Earth observations between instruments to determine inter-consistency alone cannot facilitate intercalibration unless one instrument can serve as a reference or the targets are well known. Forcing inter-consistency by relatively adjusting one or more instruments based on an inter-comparison to a single reference instrument (or an average of all instruments) yields no better accuracy than that of the chosen reference. Unless a reference instrument provides accurate, SI traceable measurements, this approach is of limited use for calibration purposes. However, simple inter-comparison and adjustment for inter-consistency can help with objectives such as seamless mosaicking of satellite imagery.

Finally, CEOS defines validation as

“... the process of assessing, by independent means, the quality of the data products derived from those system outputs” (CEOS <https://ceos.org/ourwork/workinggroups/wgcv/>).

In this sense, we consider validation as the comparison of data or measurements against remote sensing model or algorithm predictions to determine the accuracy of those predictions. With regard to independence, it is important to note, that as a rule, the exact same data or measurements used for validation must not also be used for training or calibration.

2.2 Data Product Harmonization

In the context of the SBG concept, an objective of calibration and validation in data product harmonization is to produce inter-consistent observations of the Earth's surface. To facilitate this, the SBG CVWG recommended that participating agencies keep as much information and steps in common as possible for a suite of standard data products across missions. This starts with sharing prelaunch characterization reference sources and techniques; exchanging instrument characterization data; sharing field observation data to execute validation and potential inter-calibration; establishing common standardized reference datasets and models; and identifying standard data products and algorithms. SBG CVWG also recommended that the collaborating organizations should have advanced discussions and agreements regarding work-flows, modes of communication, and conflict resolution necessary for effective collaboration towards these common resources. Ideally, resulting approaches or solutions should be reviewed by an external internationally recognized organization, such as the CEOS WGCV or similar international body.

In addition to harmonization, facilitating data product interoperability may be useful for collaborative work across agencies using common tools. The SBG CVWG recommended that these tools include transformation of data onto common spatial and spectral grids. The collaborating teams should also agree on an interoperable format and metadata. This would entail identifying and establishing a data product format including metadata that would support interoperability of all global imaging spectroscopy and multispectral TIR measurements across sensor data products, organizations, and analysis tools. The SBG CVWG recommended use of ISO data standard or CEOS protocols for development of Analysis Ready Data (ARD). Wherever possible, the collaborating teams should use standard, open source algorithms, ideally following NASA's Open Source Science Initiative, including algorithms that produce at-sensor measurement and surface radiometry and geometry. The collaborating teams should work to standardize and control the quality of reference datasets. This includes determining what, if any, reference data sets (as described earlier) should be standardized and quality controlled across collaborating missions and whether an international standard protocol, format, and metadata should be used.

The details of course are complicated. The SBG CVWG realized that the collaborating organizations and NASA would likely need to establish data agreements and corresponding government licenses to share data controlled by law. This would entail first determining what restrictions, if any, prevent or delay the timely release of instrument characterization or calibration data. Similarly, this also applies to calibration and validation data from collaborating agency's surface measurement networks or from spaceborne or airborne missions. Steps must also be taken to establish the appropriate agreements for data access and use by data product end users to assure that independent community assessment of data quality is also possible.

It is also recommended that an analysis infrastructure be established. This would involve developing computational infrastructure and analysis tools (e.g., identified through Cal/Val strategies or protocols) for comparing SBG imaging spectroscopy or thermal infrared imagery with data sets from other surface, airborne, or spaceborne sensors, as provided by collaborating agencies. Some part of this infrastructure may be developed by the community, while another portion could be developed by the collaborating missions. This would further data product interoperability and consistency of analysis. It would also further support the production of ARD, the requirement of which is currently being developed by the CEOS. NASA's Open Source Science Initiative aligns with ARD and implements policies on software, publication, and data enabling integration and improved data management, access, computing, analytics, and scientific collaboration. Such effort would facilitate capacity building, partner engagement, and incentives to help accelerate scientific discovery through open science.

2.3 Reference Data Set Management

Instrument calibration is actually implemented in the processing of data from raw telemetry to at-sensor imagery with geophysical units. That processing and the generation of downstream science data products critically depend on reference data sets and standard models. To facilitate data harmonization, it is recommended that these be standardized and version controlled, ideally across all space agencies collaborating with the SBG mission. If data products are harmonized across sensors from multiple collaborating space agencies, those organizations must agree on the metadata, format and stewardship of all of the following data sets. In addition, how reference data are archived, distributed, and configuration controlled should be planned, especially data sets that change frequently. This would likely necessitate advanced agreements or understandings and possibly shared responsibilities. Listed in Table 2 are some key examples.

Table 2

Example reference data sets and models, each supporting geometric calibration (*Geo Cal*), radiometric calibration (*Rad Cal*), surface reflectance (*Reflectance*) or the generation of certain science data products (*Science Data*), with some supporting more than one.

| Reference Data Set or Model | Purpose |
|---|------------------------------|
| Star catalog and planetary ephemeris data | Geo Cal |
| Leap second and polar wander that includes (UT1-UTC) | Geo Cal |
| Ground Control Point (GCP) database or Global Reference Image (GRI) | Geo Cal |
| Time-dependent calibration adjustments | Rad Cal |
| Lunar irradiance model (e.g., ROLO, GIRO or LIME)* | Rad Cal |
| Solar irradiance spectrum* | Rad Cal, Reflectance |
| Instrument char. data (e.g., radiometric, spectral and polarization responses) | Rad Cal, Reflectance |
| Vicarious calibration adjustments | Reflectance |
| Spectral transmission of absorbing gases (e.g., H ₂ O, O ₃ , NO ₂). | Reflectance |
| Meteorological data (e.g., wind, relative humidity, pressure and temperature) | Reflectance |
| Aerosol models | Reflectance |
| BRDF models of vicarious calibration sites | Reflectance |
| Digital Elevation Model (DEM) and Earth Gravitational Model (e.g., EGM96) | Geo Cal |
| Inland water body masks or land/water masks | Reflectance |
| Land/sea masks | Reflectance |
| Bathymetry | Reflectance, Science Data |
| Global shoreline vector data set | Science Data |
| Sea surface temperature climatology | Science Data |
| Geological and pedological map | Science Data |
| Spectral libraries | Science Data |

* - must be taken with respect to the spectral response of the instruments.

As mentioned, these data sets are important to the generation and validation of mission data products. Ephemeris and leap second data are important to accurately determine the position of

the spacecraft, which is used in geolocation and estimating solar irradiance for onboard calibration. Instrument characterization data play a role in processing calibrated TOA measurements and also for surface measurements, specifically because they can provide key information for atmospheric correction. Solar irradiance is key to generating a reflectance value and is also essential to modeling solar diffuser data for an instrument using solar calibration. It should be noted that currently, historically solar irradiance data sets have differed significantly, depending on the wavelength. It is important to use a single solar irradiance reference data set to maintain consistency (Lean et al., 2020; Coddington et al., 2019). The current recommended data set is the TSIS-1 HSRS (Coddington et al., 2020), and was accepted by the Global Space-based Inter-Calibration System (GSICS) as an international standard (Stone et al., 2021).

Most datasets listed in Table 2 that support reflectance, help facilitate atmospheric correction. BRDF models for vicarious calibration sites are used to make necessary normalization to address viewing geometry, although it is recommended that BRDF models used generally for surface reflectance be standardized to better support harmonization of surface products. Spectral libraries are important to spectroscopy algorithms, which can include apparent optical properties (AOP), such as spectral reflectance or albedo, or inherent optical properties (IOP), such as pigment-specific spectral absorption, pure and seawater spectral absorption and backscatter coefficients as a function of instrument spectral response. For contributed spectral libraries in which source spectrometers may vary and measurement protocols may differ, proper documentation of procedures and spectrometer performance should accompany shared reference data as metadata. An example of establishing shared protocols is the global community library for soils, an effort of the IEEE p4005 working group for soil spectroscopy (<https://sagroups.ieee.org/4005/>).

In addition to shared reference data or models, some ancillary or auxiliary data are necessary for algorithms, especially those employing radiative transfer models (e.g., atmospheric correction or water column modeling for benthic reflectance). These may originate from other satellite data products or models. These can include gridded data that are frequently updated, such as meteorological data or remain relatively static, such as a digital elevation model (DEM) or bathymetry.

3 Prelaunch Characterization and Calibration

Calibration begins with pre-launch instrument characterization (e.g., Polz et al., 2020) with the degree of accuracy needed dependent on the science questions or data applications that will be addressed (Thompson et al., 2021). Instrument characterization and calibration data demonstrate that an instrument is meeting performance specifications and these data are also critical to generation of datasets with geolocated, at-sensor radiometry and science products (e.g., Guanter et al., 2015; Polz et al., 2020). Some aspects of instrument characterization or calibration cannot be done well on orbit and thus we must thoroughly test each instrument under controlled laboratory conditions before launch. Some tests will be conducted at component level, while others at the instrument system level or spacecraft integrated level and these tests are performed at either ambient conditions or in a thermal / vacuum chamber, or both (Datla et al., 2011; Tansock et al., 2015). These prelaunch characterization and calibration tests also must be planned well in advance of launch. Ideally, they will follow the “test as you fly” approach (Datla et al., 2011), which posits that instruments should be calibrated as closely as possible to the same

environmental conditions expected during operation. Standard ground support equipment and calibration sources will be used to ensure traceability and repeatability.

This information includes instrument characterization data, including but not limited to, gains from radiometric calibration (e.g., response, linearity, stability, uniformity, and noise); temperature response coefficients; wavelength calibration; spectral response functions (including in-band and out-of-band (OOB) responses); polarization response; spatial response parameters; band-to-band response lags; instrument pointing data; and design-specific data (e.g., response vs scan angle, spectral ‘keystone’ or ‘smile’ features). The tests include, but are not limited to, radiometric response, dark current characterization, relative spectral response (RSR) in-band and out-of-band are all required to convert instrument counts to radiance or brightness temperatures. Radiometric response tests provide instrument gains, but also look at sensor linearity, stability, repeatability, uniformity, and noise characteristics. It is possible to combine radiometric with spectral responses using a tunable laser reference, such as SIRCUS or T-SIRCUS or the GLAMR systems. This approach provides a combined radiometric, spectral response or absolute spectral response (ASR) (Barnes et al., 2015), which potentially could reduce test cost and should be explored when designing a test plan for SBG pre-launch testing.

Additional characterization radiometric tests include polarization sensitivity, cross-talk, and near-field response and far-field stray light rejection. For polarization, instruments such as spectrometers tend to change radiometric response with the polarization state of incoming light. Typically, TOA light is polarized up to 70% across most visible and NIR wavelengths because of molecular scattering in the atmosphere (Meister et al., 2005). Variation in polarization yields a systematic radiometric artifact, which some observations are sensitive to, including dark aquatic targets. Correction of TOA measurements that are critical to the quality of aquatic observations are usually done in the atmospheric correction over water using these characterization data (Meister et al., 2005).

Additional testing of alignment, pointing, band-to-band registration (BBR), modulation transfer function (MTF), provide mostly geometric and spatial characteristics of the instrument. BBR, however, speaks also to the radiometric and spectral quality of data from the sensor, because the radiometric-spectral information from a spatially varying scene can become mixed if the bands are measured from different parts of that scene. MTF or BBR can be monitored and accounted for but cannot be improved in orbit. Therefore, pre-launch testing is crucial to understanding these characteristics.

Calibration reference elements for on-orbit calibration monitoring include space view, solar diffuser and blackbody. Most of the aforementioned data are used to convert instrument counts to radiance or brightness temperatures, adjust the wavelength scale, define bandpass of spectrometer channels, define the changes in radiometric response to thermal changes in the instrument, or support geolocation. These quantities can take different forms. For example, the radiometric and spectral characterization can be combined into a single absolute spectral response (ASR) function. Polarization and spectral responses can be used to create look-up tables used in atmospheric algorithms, especially for observation of aquatic targets. Spectral response is used to predict the solar irradiance present for each band to compute surface reflectance and as input to some atmospheric algorithms.

4 Orbit Planning - A Calibration and Validation Perspective

4.1 Calibration Opportunities with Other Missions

The SBG CVWG, in its efforts to develop a calibration concept, has placed considerable emphasis on the need to cooperate with other US and international VSWIR and TIR Earth imaging missions. One of the challenges that lies ahead for SBG and its cooperating missions, is the ability to optimize near-Polar orbiting ground tracks to image the same Earth land and aquatic regions simultaneously or near-simultaneously that minimize differences in time of observation. Such an approach facilitates relative inter-calibration opportunities between instruments and builds radiometric measurement performance confidence for the terrestrial science and application communities who depend upon both high spectral resolution and high temporal revisit frequency. This inter-calibration approach is best achieved by selecting Earth regions where simultaneous nadir observations (SNOs) or near-simultaneous nadir observations (NSOs) occur, reducing atmospheric and solar illumination angle differences, that also can align with well-established radiometric and spectral calibration reference sites (Cao et al., 2002, 2004, 2005). SNOs can be computed using online tools, such as the one found here <https://ncc.nesdis.noaa.gov/VIIRS/SNOPredictions/index.php>

To understand the effectiveness of this SBG inter-calibration approach with cooperating missions, the CVWG designed and conducted a series of NSO orbital simulations for both SBG VSWIR and TIR measurement concepts to characterize the challenges, opportunities, and limitations that can be anticipated during mission development and implementation. The objective was to leverage knowledge of existing and notational mission orbits, whether descending or ascending, and their defined parameters to simulate the possibilities for Sun-synchronous Earth imaging in an effort to constrain the proposed SBG inter-calibration approach. We used the System ToolKit™ to simulate daytime land imaging using orbital altitude, revisit frequency, and swath widths for SBG VSWIR and TIR imaging during the northern spring equinox period. The land area was covered with a 0.2° grid and coverage was computed if any portion of the swath touched the grid boundaries. We studied five specific SBG NSO scenarios with examples of potential cooperating missions.

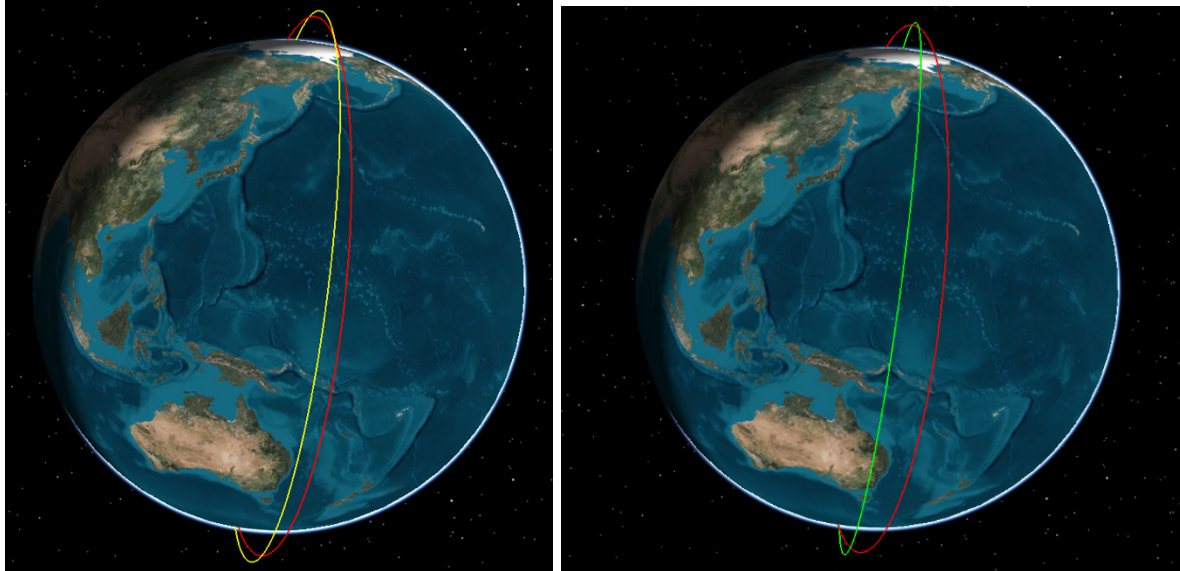


Figure 1. Equatorial crossing time (left) for Landsat 8 (green) 10:12 AM and SBG VSWIR (red) 10:45 AM; equatorial crossing time (right) for Sentinel-2a (green) 10:30 AM and SBG VSWIR (red) 10:45 AM

4.1.1 Scenario One: Crossing Time Difference between SBG VSWIR, Landsat 8, and Sentinel-2a

The SBG VSWIR reference orbit was placed at 619 km with a nadir repeating Sun-synchronous orbit (SSO) ground track at 16 days. The equatorial crossing time at the descending node was chosen to be 10:45 am local time with an instrument swath width of 185 km to ensure global observational coverage. Landsat 8 operates in a repeating SSO at an altitude of 705 km with a nadir repeat of 16 days and equatorial crossing time of 10:12 am local time. The Landsat 8 Operational Land Imager (OLI) has a 185 km swath width. The Landsat 8 OLI and SBG VSWIR instruments have an equatorial crossing time difference of more than 30 minutes as shown in Figure 1. These observations were simulated for a period of 48 days to compute NSOs occurring within 20 minutes (See Figure 2). Other intercalibration studies using NSOs have allowed longer durations between image pairs: 30 minutes in Gil et al. (2020), however 20 minutes was chosen as roughly one half of the daylight portion of an SBG orbit: time period of one SBG orbit is 97.06 minutes. The Landsat 8 OLI and SBG VSWIR NSOs occur only at high latitudes due to the differences in the equatorial crossing times. Sentinel-2a operates at an altitude of 786 km in a SSO with a nadir repeat of 10 days and an equatorial crossing at 10:30 am local time. Sentinel-2a's Multi-Spectral Instrument (MSI) has a swath width of 290 km. The SBG VSWIR and Sentinel-2a MSI observations were simulated just as done for Landsat 8 OLI. The NSOs in this comparison occur over the entire range of latitudes across the globe and are evenly spaced out (See Figure 3).

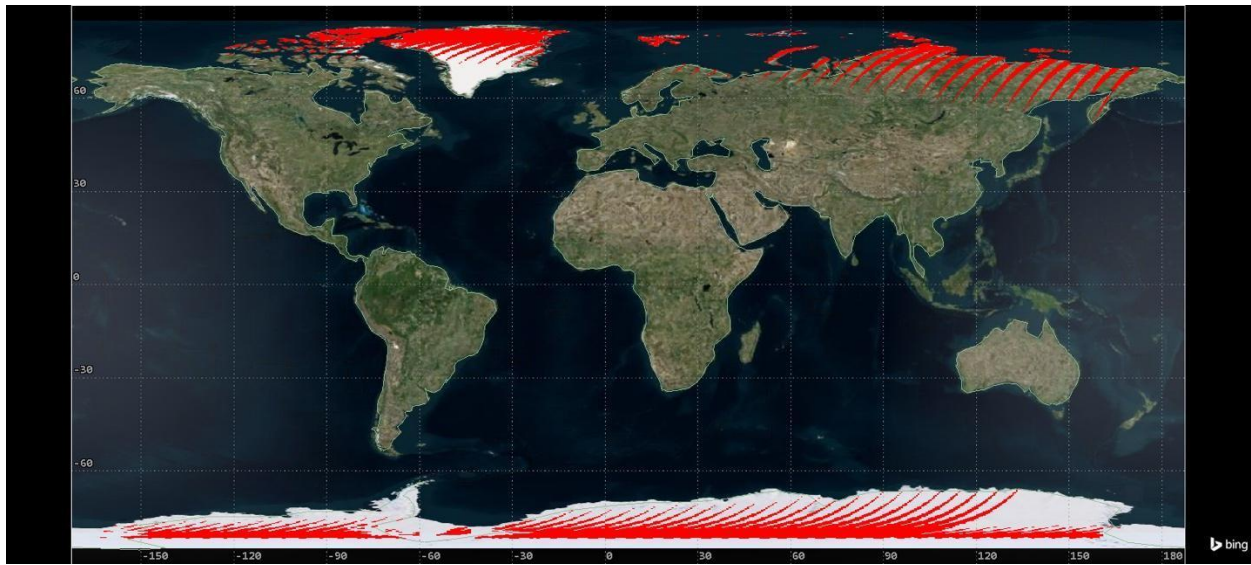


Figure 2. NSOs of Landsat 8 OLI and SBG VSWIR during a 48-day period centered on the northern spring equinox.

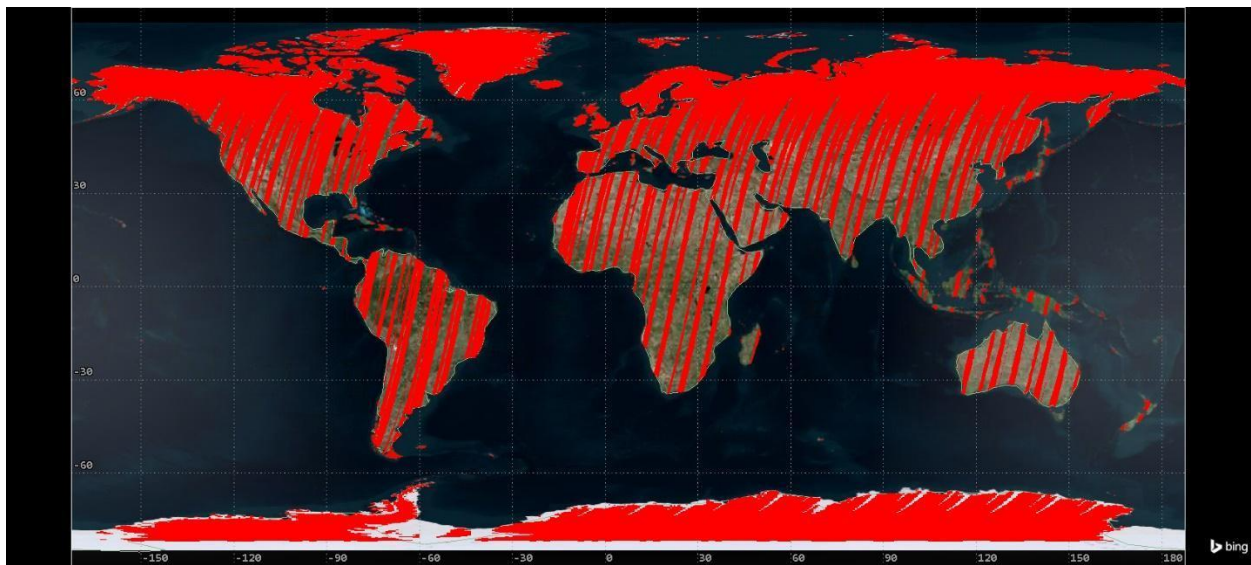


Figure 3. NSOs of Sentinel-2a MSI and SBG VSWIR during a 48-day period centered on the northern spring equinox.

4.1.2 Scenario Two: Descending SBG VSWIR and Descending CHIME

The SBG VSWIR reference orbital parameters above were used to compare NSOs occurrence with the European CHIME. The CHIME orbital altitude was specified at 632 km with an equatorial crossing of 10:45 am local time. The swath width was defined at 125 km with a 22-day SSO nadir repeating ground track. The SBG VSWIR and CHIME NSO opportunities are

shown in Figure 4 and indicate where both instruments are imaging land regions within 20 minutes of each other. This comparison shows a tendency for higher NSO coverage over higher latitudes and Polar regions, but evenly spaced NSO also occur across mid-latitude and equatorial during the 48-day period. Because SBG VSWIR and CHIME observatories are flying close in altitude, there are systematic 8 to 10 days NSO gaps in land area (Figure 5).

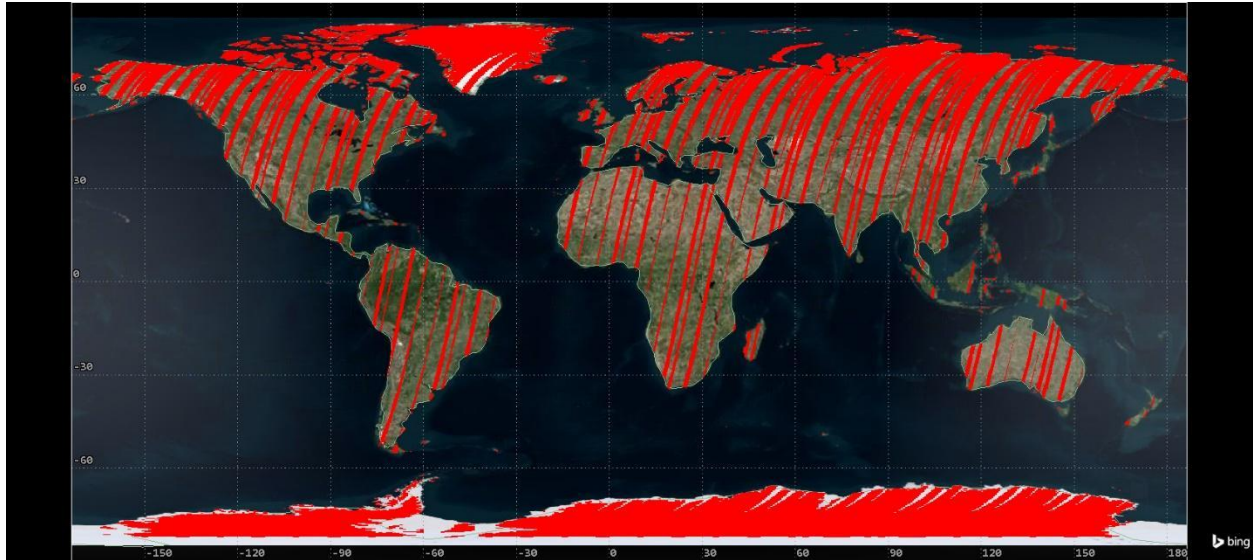


Figure 4. SBG VSWIR and CHIME NSOs during a 48-day period centered on the northern spring equinox.

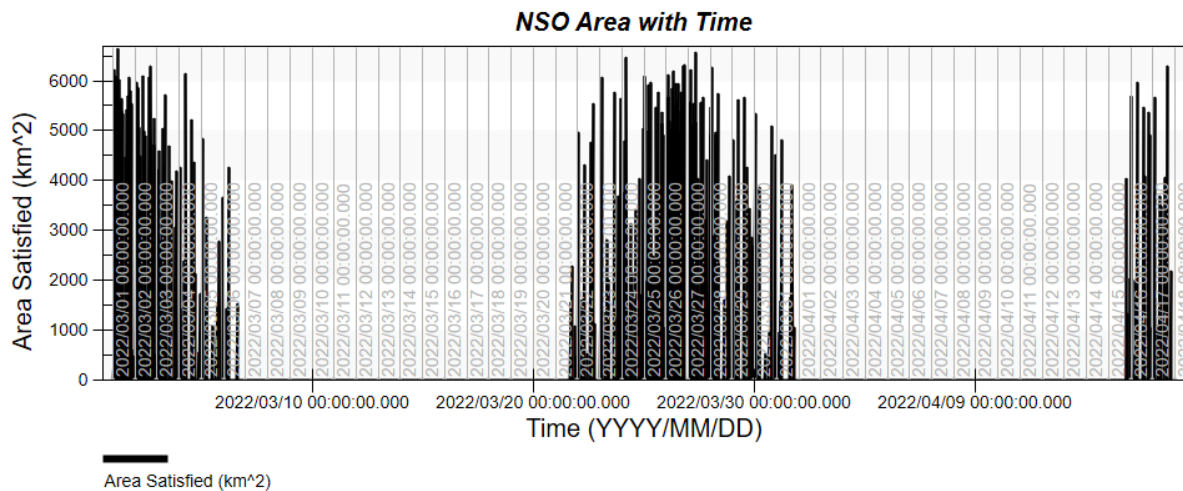


Figure 5. Periodic NSO land imaging occurrences between SBG VSWIR and CHIME missions during the 48-day northern spring equinox period.

4.1.3 Scenario Three: Descending SBG VSWIR and Ascending PACE

The SBG VSWIR reference orbit was compared with the ascending node of the Plankton, Aerosol, Cloud, ocean Ecosystem (PACE) Ocean Color Instrument (OCI) to obtain NSO's

opportunities. The PACE mission is in a SSO at an altitude of 676 km with an equatorial crossing of 1:00 pm local time. The swath width of PACE OCI is 2663 km at nadir which enables global imaging coverage at less than two days. The NSOs for SBG VSWIR and PACE OCI occur only at northern latitudes where their swath width would intersect during the daytime and Figure 6 shows the intersection of their orbital ground tracks. Figure 7 highlights NSOs between SBG VSWIR and PACE OCI at northern latitudes.

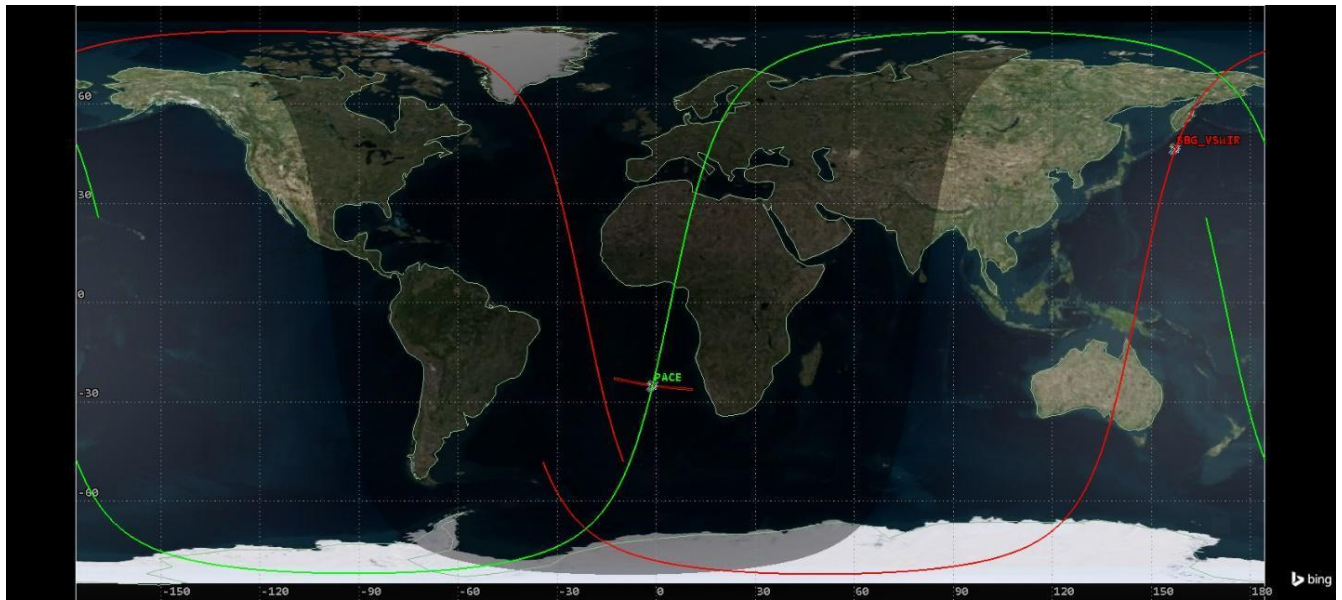


Figure 6. Ascending and descending orbit configurations for PACE (green) and SBG VSWIR (red).

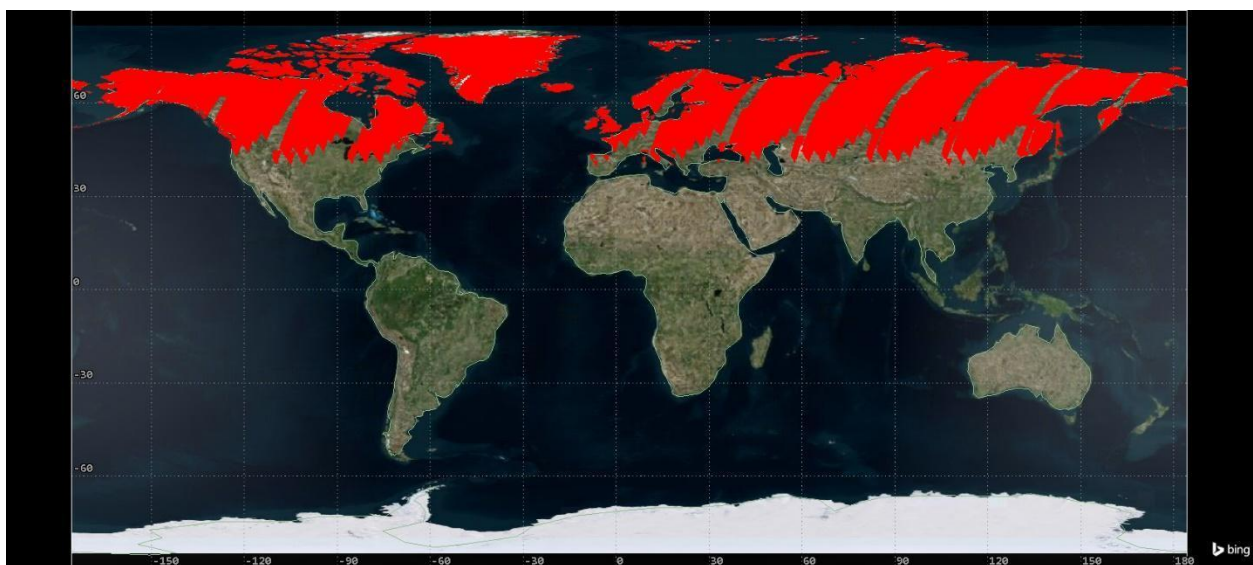


Figure 7. NSOs of PACE OCI and SBG VSWIR during a 48-day period centered on the northern spring equinox.

4.1.4. Scenario Four: Ascending SBG TIR and Descending Land Surface Temperature Mission (LSTM) TIR

The SBG TIR reference orbit was placed into a 666 km repeating ascending SSO with a nadir repeat of three days and an equatorial crossing of 1:30 pm local time. SBG TIR swath width was defined to be 935 km. The LSTM TIR orbit is at 640 km with a four-day nadir repeat descending across the equator at 1:00 pm local time with a 684 km swath width. The SBG TIR and LSTM TIR comparison was simulated for a 12-day period. The large swaths of these TIR instruments result in an increased number of NSOs across northern middle and equatorial latitudes because the time difference between observations is only 30 minutes (See Figure 8).

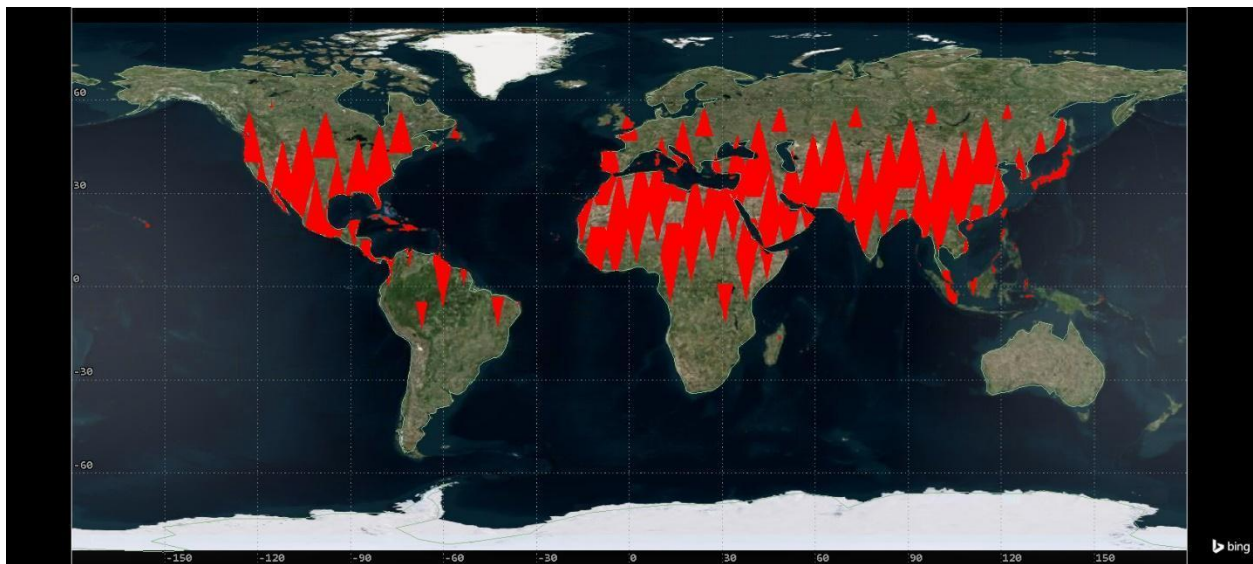


Figure 8. NSOs of LSTM TIR and SBG TIR during a 12-day period centered on the northern spring equinox.

4.1.5 Scenario Five: Descending SBG VSWIR and International Space Station (ISS) CLARREO-Pathfinder (CPF)

The SBG VSWIR reference orbit remained the same as Scenario One, Two and Three. CLARREO-Pathfinder will operate on the ISS at an altitude of approximately 400 km with an inclination of 52° while SBG VSWIR is at an inclination of approximately 98° . The orbital planes of these two missions are nearly perpendicular and result in very small areas for NSOs. The number of NSO intervals are also much less compared to two opportunities that occur in a SSO. The latitudinal coverage is also limited due the north and south 52° imaging constraint due to the ISS orbit inclination. Figures 9 and 10 show the comparison of orbit configurations and the occurrence of NSOs between CLARREO-Pathfinder and SBG VSWIR instruments over a 48-day period.

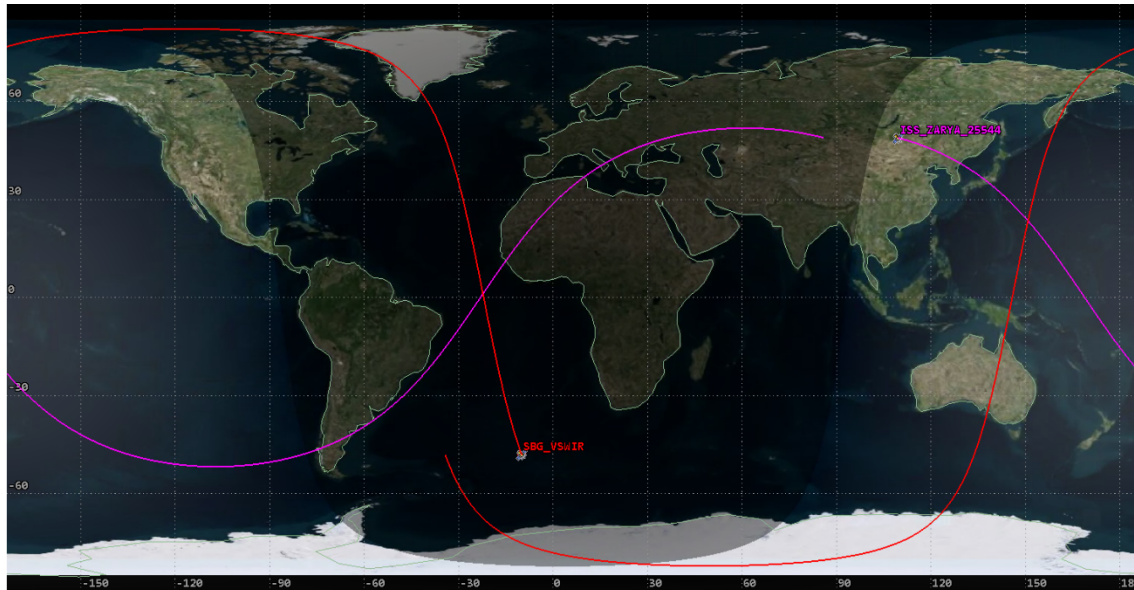


Figure 9. Descending and ISS orbit configurations for CLARREO-Pathfinder (pink) and SBG VSWIR (red).



Figure 10. NSOs of CLARREO-Pathfinder and SBG VSWIR during a 48-day period centered on the northern spring equinox.

The SBG CVWG orbital simulations for SBG VSWIR and TIR instruments reveal some key findings regarding inter-calibration among cooperating missions. First, orbital altitude, imaging revisit frequencies, and imaging swath width of existing and planned space architectures for Earth imaging clearly point out the need for more synergistic cooperation around designed SNO or NSO opportunities to maximize cross-mission capabilities if inter-calibration is a strategic mission priority. Second, there clear geographic imaging patterns that emerge across the global

domain based on the current portfolio of existing and planned US and international VSWIR and TIR measurements, and while these occurrences may result in ad-hoc science and application utility, the current identified NSO maybe not align very well with the established ground-based radiometric calibration reference sites that are currently used in terrestrial remote sensing calibration and validation. Finally, SSO equatorial crossing times that exceed 20-minute NSO intervals, coupled with orbital ground tracks of the same revisit frequencies provide very limited inter-calibration opportunities except for high latitude including Polar regions. The SBG CVWG recommends better mission cooperation between US and international space agencies to optimize orbits in support of inter-calibration and higher quality terrestrial remote sensing science and application data products. This would require a balance between facilitating some simultaneous observations, while maintaining a sufficient offset to improve temporal sampling of the combined observations. This could be accomplished by choosing orbits with different revisit times that provide occasional alignment.

4.2 Orbit Planning for Geometric Characteristics

The VSWIR imaging spectrometer and a TIR imager are planned to fly in a late morning and an early afternoon, sun-synchronous, retrograde, integer-day ground track repeating near-polar orbiting satellite. On-orbit operations through regular drag make-up and inclination adjust maneuvers will maintain orbit altitude, eccentricity, inclination, local time at ascending or descending node, ground track repeatability accuracies to within tight margins (Bilimoria and Krieger, 2011). The instrument designs will take the earth rotation, inclination angle, and variations of altitude and satellite speed along the sub-satellite point track into account so that ground coverage from the instruments will not have underlaps in either the cross- or along-track direction (Lin et al., 2016; Lin et al., 2018; Lin et al., 2019).

5 Inter-Calibration and Monitoring

5.1 Commissioning and Long-Term Monitoring

After the satellite is launched into an initial orbit altitude, there will be a series of orbit raising and inclination adjustment maneuvers to attain the nominal planned orbit altitude and inclination. In the meantime, an early orbit check-out (EOC) campaign will be conducted. That includes activation of GPS receivers, attitude determination and control sub-system, and possibly instruments, among others. This can include testing of onboard calibration systems, such as lamps or a blackbody source (after thermal detectors have been adequately cooled). After EOC, an intensive calibration and validation (ICV) campaign follows. The ICV establishes a baseline of calibration coefficients. During this phase, any onboard solar calibration system can be tested and further characterized in orbit using spacecraft maneuvers that move the Sun across these solar calibration system field-of-view. For example, primary EnMap calibration will be done using onboard systems (Wilkens et al., 2016) while validation will rely, in part, on the cooperation with experienced international partners, and data from established calibration, validation and monitoring sites and networks detailed in following sections, as well as on intercomparison of data from other missions (Brell, et al., 2021). Long-term monitoring corrects for drifts of calibration coefficients. Periodic ICVs may establish updates to calibration, for example, Masek et al., 2020, describe a combination of sensor intercomparisons, use of the AEROSOL ROBOTIC NETWORK (AERONET), Surface Radiation Budget Network (SURFRAD), and

buoy networks, and comparison with field spectroscopy and airborne imaging spectrometer data to validate Landsat Level-2 surface reflectance and surface temperature products.

To harmonize data sets from multiple missions, intercalibration on-orbit using common references is critical. The Moon can potentially facilitate intercalibration target over long periods of time, provided current efforts successfully improve models of lunar irradiance to become SI traceable and <1% accuracy or better (Stone et al., 2021). It is potentially an ideal target because its measurement is not influenced by the Earth atmosphere or anything that can be significantly influenced by changes in the Earth's climate (this is discussed further in the next section). Observations of the Earth with near identical timing and geometry could also support true inter-calibration in the short term provided the surface target is well known at the top of the atmosphere (e.g., the target has a very predictable Bi-Directional Reflectance Distribution Function (BRDF) and the atmospheric optical column above the target is accurately measured and modeled). However, atmospheric effects could be influenced by long-term climate changes and thus limit the Earth as an ideal target for long-term intercalibration for high levels of accuracy.

Achieving radiometric scale agreement between instruments not only depends on the quality of the radiometric knowledge of the reference observation, but accuracy of the spectral and geometric calibration. Errors in wavelength positions of spectral channels can translate into radiometric errors (depending on the slope of the reference spectrum with respect to wavelength). Misaligned imagery can likewise lead to radiometric errors (depending on the radiometric partial derivatives of the image with respect to raster dimensions). Therefore, it is first important to address the spectral and geometric calibration using common references before intercalibration and data harmonization requires a common spatial and spectral grids.

Spectral calibration can be monitored on-orbit using onboard reference sources (Micijevik, et al., 2022) or external reference targets. External references could include gas absorption lines caused by the Earth's atmosphere (Green et al., 2003; Richter and Schlapfer, 2019). In addition, minerals with strong, narrow absorption features at the Earth's surface could also serve as spectral calibration targets. Examples of such targets include the long utilized geologic remote sensing reference site at Cuprite, NV (Swayze et al., 2014) and the site at Makhtesh Ramon, Israel (Pearlshtien et al., 2021; Pearlshtien and Ben Dor, 2022). Fraunhofer lines appear in lunar or solar observations, in cloud and ice reflectance, or in specular reflectance off water. But the spectral features of the solar spectrum are too fine-structured to adequately resolve given the SBG VSWIR expected 10 nm spectral resolution over its 400 to 2500 nm range (see Figure 11). However, as demonstrated in Figure 11, the SBG VSWIR spectrometer could perhaps use atmospheric absorption features to monitor, which would be observed for bright targets on Earth.

Reference features in spectra, such as absorption lines, are well defined by well-known laws of physics, are very predictable and so instrumentation or modeling is less necessary for target sites on the Earth's surface. Geometric calibration of the instrument line-of-sight can also be refined in orbit during the commissioning phase using surface features such as narrow bridges, established reference ground control targets, or even high-resolution reference imagery such as digital orthophoto quadrangles (DOQ). However, radiometric calibration is more challenging because most potential calibration targets found on the Earth's surface are subject to some degree of change (and changing reflectance or temperature are characteristics of very phenomena that

we seek to measure!). Finding stable, well-known references for the radiometric scale can hence be especially challenging.

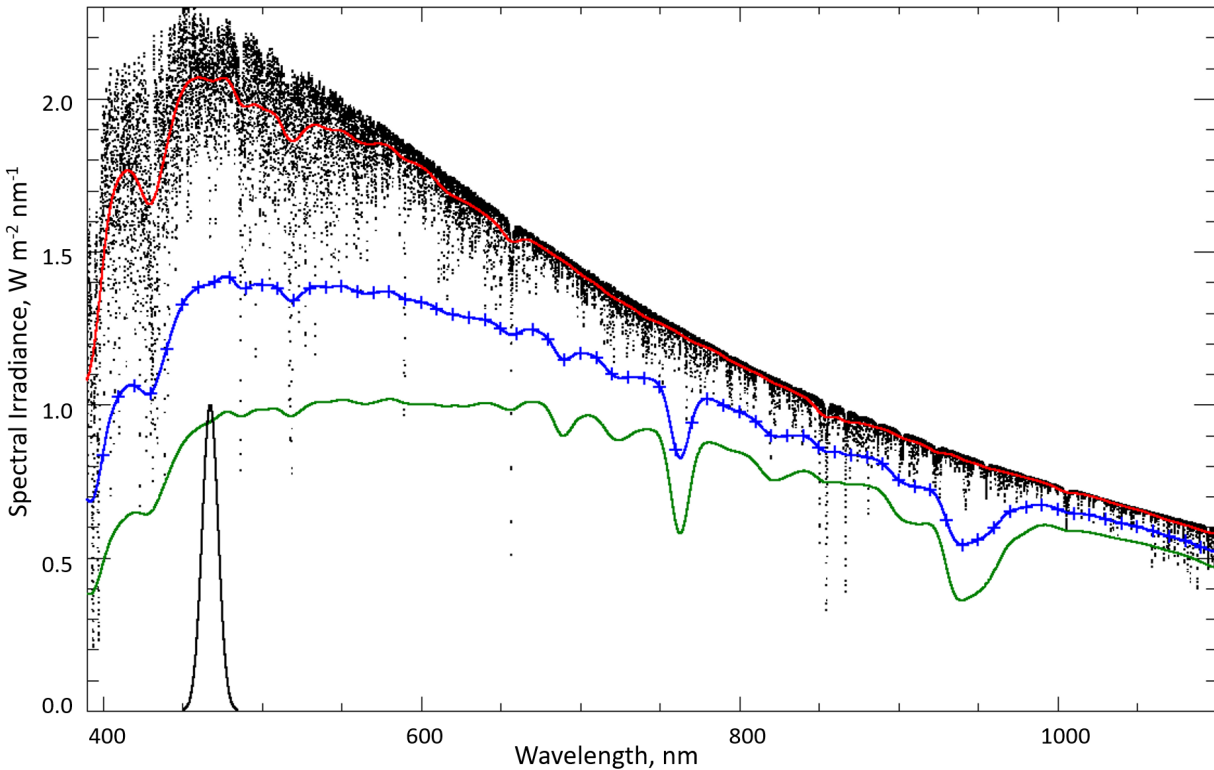


Figure 11. Simulated SBG spectra. Dots are the TSIS-1 Hybrid Solar Reference Spectrum (HSRS) solar spectrum at 0.1 nm resolution (Coddington et al., 2021), showing most of the solar structure. Fraunhofer lines are about 0.4 nm wide, e.g., H α at 656. The colored lines show simulated measurements by convolving with a Gaussian shape with a nominal FWHM of 10 nm. The black line near 470 nm shows the 10-nm spectral response profile used. The red line is a simulated measurement of the exo-atmospheric solar irradiance spectrum. The blue line simulates the same measurement of exo-atmospheric solar irradiance after one pass through a typical atmosphere over-land atmosphere based on MODTRAN (Anderson, 2000); the plus signs indicate nominal bands at 10 nm spacing. The green line simulates the same measurement with two passes through the same modeled atmosphere.

Vicarious calibration involves special *in situ* data (not used for validation) to characterize the satellite sensor response. Much of the same or similar *in situ* instrument infrastructure is used for acquiring these data. As with validation, the calibration plan should also leverage existing best practices, resources, techniques, and protocols. Vicarious calibration also typically requires modeling to provide TOA radiance or reflectance to compare against satellite observations. This means that a vicarious calibration plan must have input from the ground systems to be sure to use the same radiative transfer model that is being used operationally for atmospheric correction.

5.2 The Moon

Using the Moon as a full-system measure of responsivity changes for solar reflectance bands of on-orbit instruments has been a common and generally successful activity for the past quarter-century. Three major steps are involved: 1) acquiring an image of the Moon in all solar-reflective bands; 2) processing the image data to an apparent lunar irradiance; 3) comparing the measured irradiance to a spectral-irradiance model of the Moon. Each of these steps has challenges, often unrecognized, which has limited the effectiveness and the acceptance of lunar calibration. These challenges are rapidly being addressed and lunar calibration in the SBG era holds the promise of sub-percent absolute calibration and trend capability (Stone et al., 2020; Kieffer, 2022).

The Moon can be considered a reference diffuser of accurately known size, with sharp edge on half its circumference, zero background and weak broad spectral features. Its reflectance is similar to soil. The stability of its overall reflectance (10^{-8} / annum (Kieffer, 1997) is better by several orders of magnitude than artificial surfaces. However, lunar irradiance varies widely with geometry and a model is required; this relation is conceptually knowable to great accuracy and precision. Total lunar spectral irradiance for a given set of illumination and viewing angles and distances can be modeled empirically based on prior lunar irradiance characterization as a function of geometry. Such a lunar spectral-irradiance model (Kieffer and Stone, 2005) has been in common use for nearly two decades, and improved models are an active research area (Stone et al., 2020; Taylor et al., 2021; Wang et al., 2020; Sun and Xiong, 2021; Kieffer, 2021a; Kieffer, 2022) Lunar irradiance is polarized (Dollfus, 1962), up to several percent at common calibration geometries, passing through zero at phase angles near 24° . Polarization has been largely ignored in lunar calibration to date, but modern measurements (see <http://calvalportal.ceos.org/lime-documents>) are being made after nearly a century gap.

Lunar calibration observations are best made by pointing the instrument directly at the Moon, using the same optical configuration as science observations. This commonly involves a spacecraft attitude maneuver and places requirements on spacecraft agility. A mission concept should plan on lunar observations dense in commissioning, then each month for at least a year, then becoming spaced out; also, soon after any traumatic event on the spacecraft.

At present, lunar-calibration results differ substantially between many instruments (Kieffer, 2021b). The main suspect is differences in optical path between lunar calibration and normal science observations; these must themselves be periodically calibrated by direct observations of the Moon. Because the Moon is static, a lunar observation at any time, even years ago, can be used for a radiometric calibration and benefit from improving lunar models. E.g., an entire constellation could calibrate on the Moon with no simultaneity requirements.

Possible indirect effects of an attitude maneuver can be determined during commissioning; e.g., long scans crossing the Moon at several azimuths, scans in both directions, observations early and late along an orbit and early and late in an attitude maneuver. It is important to be prepared for near-real-time analysis in case of unexpected artifacts, allowing them to be pursued during commissioning.

Lunar observations also aid geometric assessments; lunar images are unparalleled for the identification of 'ghosts'; bright-limb scans can track any degradation of MTF, the virtual zero

background allows sensitive determination of off-axis response and quantifying the size-of-source effect, which is very difficult in the laboratory.

5.3 The Sun

The Sun can serve as a source for calibrating instruments in flight. Like the Moon, it can facilitate both an absolute calibration of the instrument after the transfer to orbit and monitor the instrument calibration, supporting time-dependent calibration. The sun has the advantage of being relatively stable over the VSWIR range to about one part in a thousand (Lean et al., 2020; Coddington et al., 2019) and with the more accurate knowledge of the solar spectral irradiance provided by the TSIS-1 HSRS (Coddington et al., 2021), the solar output has become a more accurate reference. Unlike the Moon, the Sun does not go through large changes that must be carefully predicted and it can be viewed anytime.

However, the main challenge of using the Sun is that it is several orders of magnitude brighter than the targets that Earth observing satellites are designed to observe. This is typically addressed by adding an optical element to step down the solar output before being observed by the instrument. A common approach is to use a uniform, isotropic reflective plate, called a solar diffuser. Diffusers can be spectrally near white or doped to be gray, further stepping down the solar signal. Doping can also add spectral features that can be used to monitor the spectral calibration of spectrometers on orbit, provided they have sufficient spectral resolution. Solar diffusers can be constructed of Polytetrafluoroethylene (PTFE), and come in different levels of purity. Other diffuse materials or coatings can also be used, such as ceramics, Quartz Volume Diffuser (QVD) or barium sulfate.

However, there is a key drawback with such a calibration system: the reflectance of the solar diffuser is not constant, but changes with exposure to the harsh environment of space and strong solar irradiation. These changes differ with material and manufacture. In all cases, a strategy to monitor the changes to the solar diffuser is critical to avoid the introduction of spurious trends in the Earth observations. One method to quantify changes to the diffuser in space is to situate a monitoring instrument to compare the solar diffuser at a similar viewing geometry to what the main instrument sees during calibration and ratio that to light from the Sun attenuated with a screen. These devices are called Solar Diffuser Stability Monitors (SDSM) and have been used for the MODerate resolution Imaging Spectroradiometer (MODIS) and the Visible Infrared Imaging Radiometer Suite (VIIRS) instruments. However, these instruments must be well characterized and stable or they will leave residual spurious trends in the solar time-dependent calibration. Another approach to the SDSM is to use two or more solar diffusers, one for frequency observation and another to be shielded and removed for observation much less frequently. The less frequently observed diffuser provides a baseline against which the more frequently observed diffuser can be compared and its changes monitored and removed from a time-dependent calibration. This approach will be used by the upcoming OCI ocean color spectrometer in the PACE mission.

Also, unlike the Moon, because the solar diffuser can provide broad uniform and isotropic source across the entire IFOV of the instrument, detector arrays can be checked for striping, depending on the instrument design. However, because exposure to solar radiation over time may not be consistent across the diffuser (or if there are any flaws in manufacture), the solar diffuser may

not degrade uniformly, thus changing into a nonuniform or anisotropic source. There is no current design to monitor or accurately detect such phenomena, which could undermine characterization of differences between detectors.

5.4 The Earth

The SBG CVWG recommends that the NASA SBG project and its collaborating agencies identify or develop joint surface measurement networks. This would start with the identifications of existing resources for validation or vicarious calibration data and determining any potential gaps or limitations. The agencies should work to share development of any additional resources needed and should also identify any airborne and spaceborne resources for calibration and validation of imaging spectroscopy or thermal infrared imagery. For surface, airborne and spaceborne assets, the NASA SBG project and its collaborating agencies should leverage current and emerging methods by identifying existing or developing new standard validation and vicarious calibration strategies and protocols. In this section, we consider some key examples for calibration and validation measurement resources on the Earth's surface.

Masek et al., 2020, recommended that efforts to characterize and validate Landsat Level-2 data products expand to beyond bright surfaces with dry atmospheres to regions where atmospheric compensation is more challenging to implement, and to bright and dark land surface targets beyond just deserts and vegetation (e.g., water bodies, bare soil, snow and ice, and impervious surfaces). To that point, EnMap will validate surface reflectance with *in situ* reference measurements from selected, diverse core sites that span agricultural, aquatic, exposed geologic, and snow-covered surfaces (Brell et al., 2020). Because potential variation in the Earth's atmosphere increases uncertainty, care must be taken to avoid adjusting a time-dependent calibration as a result of atmospheric variations. For this reason, onboard or celestial references are preferred for calibration (Storch et al, 2014), especially with mission objectives such as change detection, monitoring, and trending, while vicarious measurements are employed for validation of data products (Masek et al, 2020). On the other hand, for aquatic remote sensing, vicarious calibration is primarily used to optimize accuracy of surface radiometry, not at-sensor accuracy, so biases in the atmospheric radiative transfer model are incorporated in the adjustments applied to the production of water-leaving reflectance (Clark et al., 1997). For terrestrial applications, vicarious calibration has been used to evaluate and if necessary, adjust surface reflectance values retrieved through a radiative transfer algorithm (Mairersperger et al., 2013; Clark et al., 2002).

5.4.1 Terrestrial References

To characterize radiometric response of optical remote sensing systems, a number of tools and techniques are utilized, including PICS, RadCalNet, SURFRAD, AERONET and instrumented thermal calibration sites.

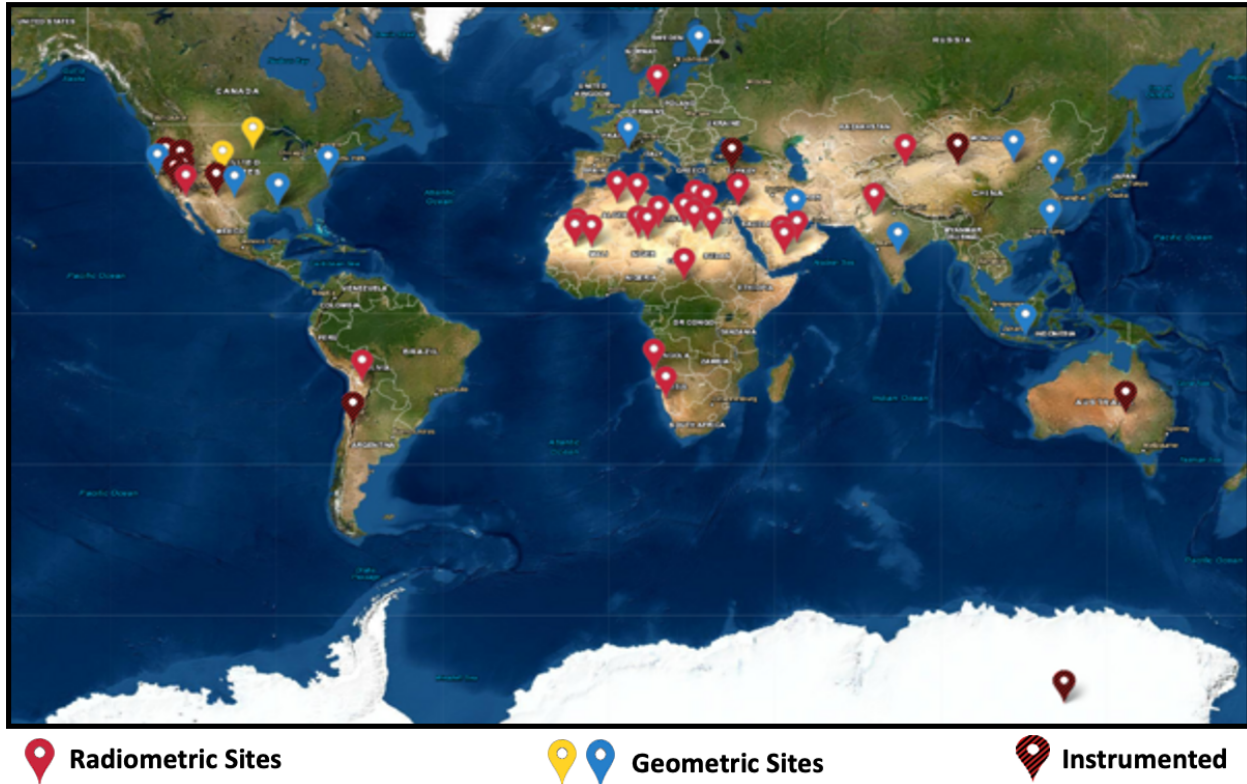


Figure 12. Global distribution of CalVal sites maintained by USGS (<https://www.usgs.gov/tools/test-sites-catalog>) used in Landsat (Both yellow and blue pins are geometric sites, where blue pins are specifically for spatial resolution tests).

5.4.1.1 Radiometric Calibration Targets

Terrestrially, PICS are locations that are found to be highly radiometrically stable over time (Table 3). PICS of highest stability include flat sandy desert terrain, where geometric relief, atmospheric and surface moisture as well as population and human-induced change are all minimal. Other areas, such as inland ice sheets have been investigated and used on occasion for specified purposes. The general geographic distribution of candidate PICS can be seen in Figure 12. However, these locations can be impacted by adverse radiometric, spectral and thermal characterization conditions including metamorphosing surface, i.e., change in snow grain size and ice structure, poor illumination angle, solar geometry and increased atmospheric dynamics. At desert sites, spectral response and repeatability nominally measure within 1-3% depending on spectral band, viewing geometry and site (Cosnefroy et al., 1996; Helder et al., 2013). The CEOS WGCV has agreed upon and endorsed a set of six such desert PICS for long-term satellite monitoring and reference purposes, and more information can be found at https://calvalportal.ceos.org/pics_sites and within the PICS reports published therein. New PIC usage methodologies and techniques in evaluation stages include extended PICS (EPICS) and super or cluster PICS with the goal of increasing PIC scene analysis data (e.g., Vuppula, 2017; Khakurel et al., 2021).

The Aerosol RObotic NETwork AERONET program (<https://aeronet.gsfc.nasa.gov>) was established by NASA and the Université de Lille Laboratoire d'Optique Atmosphérique in the early 1990s. The program characterizes and monitors aerosols, water vapor and clouds at discrete

calibration sites around the globe. The network provides openly available, long-term continuous data for use by several remote sensing missions, data products, airborne campaigns and similar uses (Holben et al., 1998). The program continues to evaluate, curate data and expand stations over time.

The RadCalNet (<https://www.radcalnet.org/>), an initiative of CEOS WGCV, is a network of radiometric calibration sites across the globe providing SI-traceable spectrally-resolved TOA reflectances including associated uncertainties to aid in-flight and on-orbit radiometric calibration and validation of Earth observation sensors operating in the (VSWIR) spectral region (Table 3). Currently, there are five such sites (two in China and one each in France, Namibia, and the USA) equipped with automated ground instruments making continuous measurements and are managed independently. The RadCalNet attempts to improve the temporal sampling issues that exist in the on-orbit sensor calibration, provides global consistency, and increases the available calibration opportunities, by networking measurements from these sites. Bouvet et al., 2019 provides further information on data collection including their data processing approach and an example of inter-consistency study between two sensors using RadCalNet data. Alonso et al., 2019, describes the use of RadCalNet measurements in the validation of DESIS imaging spectrometer data. In addition, Czapla-Myers et al., 2020 discussed results of comparing several space-borne sensors using one of the RadCalNet sites located at Railroad Valley, Nevada, USA also known as Radiometric Calibration Test Site (RadCaTS).

The NOAA Global Monitoring Laboratory provides the Surface Radiation Budget (SURFRAD) Network of hourly Earth and atmosphere system radiation measurements across a wide network of stations in varying geographic and climate zones (<https://gml.noaa.gov/grad/surfrad/>). The program was established in the early 1990's with the aim of providing reliable field data to support remote sensing climate research. Primary measurement variables include upwelling and downwelling radiation, direct and diffuse solar, photosynthetically active radiation, UVB, spectral solar and ancillary meteorological parameters (NOAA Earth System Research Laboratory, 1995).

The recently launched Landsat 9 and soon to be launched EnMap include plans to utilize contributed data from collaborators across the globe for validation during a commissioning phase. The utilization of contributed data from various sources places a secondary calibration/validation burden on the teams collecting field-measured data. Spectrometer characterization (spectral and radiometric) and measurement protocols should be established to ensure equitable data, for example, Malthus et al., 2019; Ong et al., 2018. However, the measurement protocol may vary between surface types, for example, water bodies versus bright soil or sediment surfaces. The recently deployed FLARE network is a commercial system of satellite validation of geometric and radiometric performance (Durell and Russell, 2020).

5.4.1.2 Thermal Calibration Targets

Thermal emissive band calibrations are completed in addition to the solar reflective band calibrations. In contrast to the solar reflective region of the electromagnetic spectrum, thermal infrared energy observed by satellites is a measurement of Earth surface emitted radiance, as well as energy absorption and emission through the atmosphere (Czajkowski et al., 2000). Thermal emissive band calibration typically involves on-board blackbody observations and use of Earth

surface aquatic and terrestrial calibration data (Hook et al., 2007; Xiong, 2009; Pérez Díaz, et al., 2021). Many current and forthcoming thermal Earth observation missions have used the long-term automated and complimentary thermal infrared calibration sites, for example at Lake Tahoe, CA/NV, USA and Salton Sea, CA, USA (e.g., Hook et al., 2020) (Table 2) and end-member high and low temperature or emissivity targets for calibration and validation purposes (e.g., Hall et al., 2008). Calibration and validation efforts typically use ground instrument measurements of thermal emitted surface radiance, atmospheric observations and a radiative transfer model to simulate the at-sensor equivalent thermal radiance values. These at-sensor simulated thermal radiances are then compared with actual on-board sensor measured radiance and assessed by thermal spectral band. Hulley et al., 2022, describe two primary methods for validation of land surface temperature and emissivity products, the classical Temperature-based approach (Wan et al., 2002) relying on instrumented sites and the Radiance-based method (Coll et al., 2009) applicable where emissivity is known, which were applied to ECOSTRESS data for fourteen land and water sites located in North America, Europe, and Africa. An international team of experts representing the CEOS WGCV have recommended two additional methods, multisensor intercomparison and time-series analysis approaches (Guillevic et al., 2018) which are useful for comparing products generated from different algorithms and with different observational characteristics, and for observing long-term trends, biases, and atmospheric effects.

Table 3
Global Terrestrial Sites for Vicarious Calibration

| Site Name | Location |
|-------------------|-----------------------|
| Algeria 3 | 30.32°N, 7.66°E |
| Algeria 5 | 31.02°N, 2.23°E |
| Arabia 1 | 18.88°N, 46.76°E |
| Arabia 2 | 20.13°N, 50.96°E |
| Baotou Sand* | 40.8517°N, 109.6289°E |
| Barreal Blanco* | 31.86°S, 69.45°W |
| Demmin | 53.90°N, 13.17°E |
| Dome C* | 74.50°S, 123.00°W |
| Dunhuang* | 40.13°N, 94.34°E |
| Egypt 1 | 27.12°N, 26.10°E |
| Ivanpah Playa* | 35.5692°N, 115.3976°W |
| La Crau* | 43.56°N, 4.86°E |
| Lake Tahoe*† | 39.0°N, 120.0°W |
| Libya 1 | 24.42°N, 13.35°E |
| Libya 2 | 25.05°N, 20.48°E |
| Libya 3 | 23.15°N, 23.10°E |
| Libya 4 | 28.55°N, 23.39°E |
| Lunar Lake Playa* | 38.40°N, 115.99°W |
| Makhtesh Ramon* | 30.59°N, 34.84°E |
| Mali | 19.12°N, 4.85°W |
| Mauritania 1 | 19.4°N, 9.3°W |

| | |
|------------------------|----------------------------|
| Mauritania 2 | 20.85°N, 8.78°W |
| Namib Desert 1 | 24.98°S, 15.27°E |
| Namib Desert 2 | 17.33°S, 12.05°E |
| Negev* | 30.11°N, 35.01°E |
| Niger 1 | 19.67°N, 9.81°E |
| Niger 2 | 21.37°N, 10.59°E |
| Niger 3 | 21.57°N, 7.96°E |
| Railroad Valley Playa* | 38.5°N, 115.69°W |
| Rogers Dry Lake* | 34.96°N, 117.86°W |
| Salton Sea*† | 33.22532°N, 115.82425°W |
| Sonoran Desert | 32.35°N, 114.65°W |
| Sudan 1 | 21.74°N, 28.22°E |
| Taklamakan Desert | 39.83°N, 80.17°E |
| Thar Desert | 27.63°N, 71.86°E |
| Tinga Tingana* | 29.00°S, 139.86°E |
| Tuz Golu* | 38.83°N, 33.33°E |
| Uyuni Salt Flats | 20.38°S, 66.95°W |
| White Sands* | 32.92°N, 106.35°W |
| Yemen Desert | 16.87°N, 47.55°E |

*Currently Instrumented, †Thermal Site.

In thermal calibration and validation activities, water vapor is an important quantity that must be well characterized (e.g., see Quattrochi and Luvall, 2004 and Xiong et al., 2020 for more details). Thermal emissive bands also must be well-calibrated for the ‘split window’ data algorithm technique which utilizes the difference in brightness temperature between targeted thermal emissive bands to correct for atmospheric effects as compared to measured Earth aquatic and land surface temperatures.

5.4.1.3 Geometric Calibration and Assessment

Instrument geolocation calibration starts when the first light images become available, even before the nominal orbit altitude is attained. It is expected that the initial correction will be very large, in the order of thousands of microradians in the instrument-to-spacecraft mounting alignment angles that are thousands of meters on the ground, due to installation uncertainty and launch shift (Storey et al., 2014; Lin et al., 2018). It is also expected that the mounting coefficients will be fine-tuned before the end of commissioning using selected high accuracy, cloud-free ground control points derived from USGS Digital Orthophoto Quadrangle (DOQ) data (Kieffer et al., 2008; USGS 2018) for SBG sensors, similar to those used for Landsat (Storey et al., 2014).

Long-term monitoring of geolocation accuracy assessment also uses the Global Land Survey (GLS) (Gutman et al., 2013; Rengarajan et al., 2015), in addition to regional USGS DOQ ground control points. If significant drifts occur, re-processing of data collections is required by applying temporal pointing variations (Storey et al., 2014; Lin et al., 2020). Landsat 8 has achieved

geolocation accuracy of 18 meters of circular error at 90th percentile (CE90) (Storey et al., 2014) in data Landsat Collection 1. After Sentinel-2 from the European Space Agency (ESA) was launched in June 2015, a global reference image (GRI) database was generated (Dechoz et al, 2015; Clerc et al, 2021). The Landsat 7 GLS database was augmented with Landsat 8 data, which was further harmonized with GRI with space-based triangulation (Storey et al, 2019). Reprocessed Landsat collection 2 of Landsat 8 data has achieved geolocation accuracy of 8 meters at CE90 using GCPs from the harmonized GLS (Rengarajan et al, 2020). The accuracy is achieved by registering level-1 products to the control base of GRI and Landsat 8 augmented GLS (USGS 2021).

The ground sampling distances (GSDs) for SBG are expected to be 30 m and 60 m for the VSWIR sensor and TIR sensor, respectively. Sentinel-2 has three GSDs, 10, 20 and 60 m. Landsat 8 has GSDs at 30 m for visible, near-infrared, and short-wave infrared bands, 100 m for thermal bands, and 15 m for a panchromatic band. Because the GSDs for Landsat and Sentinel-2 are comparable to SBG, SBG can employ the same geometric calibration methods and achieve similar sub-pixel geolocation accuracy.

The geolocation accuracy assessment will include the effects from focal length deviation. If the focal length deviates from the nominal designed value, it should be corrected by putting the focal length as a geolocation parameter in a look-up table (Tilton et al., 2019; Seo et al., 2016; Wang, et al., 2014).

Geolocation calibration is a major part of instrument on-orbit geometric calibration and assessment. Other parts include MTF and BBR characterization. MTF and BBR calibration activities are performed in prelaunch tests (Knight and Kvaran, 2014; Lin et al., 2011). On-orbit MTF assessment may be performed using lunar observations (Choi et al., 2014; Wang et al., 2015), Earth surface target (Tilton et al., 2017a), or special setup on the ground (Wenny et al., 2015), see Table 4. On-orbit BBR assessment may be performed similarly using lunar observations (Wang et al 2015) and Earth surface targets (Tilton et al., 2017b; Tilton et al., 2019).

Note that instrument geolocation performance highly depends on the performance of spacecraft ephemeris (position and velocity) and attitude. Loss of pointing accuracy occurs during orbit management in drag make-up and inclination adjust maneuvers and after these maneuvers. It is important to understand the impacts of these maneuvers on the quality of instrument data products.

Table 4

Global Sites for Geometric Calibration

| Site Name | Location |
|-----------------------|---------------------------|
| 1 mi Road Grid | 42°N, 96°W, extended |
| Baotou | 40.8517°N, 109.6289°E |
| Big Spring | 32.220436°N, 101.512524°W |
| Chesapeake Bay Bridge | 37.034342°N, 76.079861°W |
| FGI Sjukulla | 60.2421°N, 24.3838°E |
| Jiaozhou Bay Bridge | 36.152706°N, 120.221456°E |

| | |
|--------------------|---------------------------|
| King Faud Causeway | 26.1961°N, 50.342°E |
| Lake Pontchartrain | 30.2125°N, 90.1219°W |
| Peng Hu | 23.519989°N, 119.583581°E |
| Pueblo Range | 38.2827°N, 104.6066°W |
| Salon de Provence | 43.6061°N, 5.12°E |
| San Mateo Bridge | 37.600958°N, 122.209033°W |
| Shadnagar | 17.034249°N, 78.183060°E |
| Sioux Falls Range | 43.555562°N, 96.745806°W |
| Stennis | 30.3855°N, 89.6285°W |
| Suramadu Bridge | 7.179025°S, 112.780693°E |

When the SBG TIR instrument data is used in combination with the SBG VSWIR instrument data, the finer resolution VSWIR data will be re-sampled to the coarser resolution TIR location. The re-sampler will be designed such that the MTF of the re-sampled VSWIR data is compatible with the MTF of the TIR data. Similar re-sampler(s) should be designed to combine other instrument data for higher level downstream data product generation.

5.4.2 Aquatic Targets

To support remote sensing of coastal and inland aquatic waters, a number of calibration and validation resources are used for accurately calibrating the TOA satellite observations. In addition to lakes mentioned under terrestrial targets (section 5.4.1.2), additional networks and measurements across the open ocean help to facilitate thermal calibration. Regarding surface reflectance in the visible wavelengths, other sites include the Marine Optical BuoY (MOBY), BOUSSOLE, WATERHYPERNET, and the Aerosol Robotic Network - Ocean Color (AERONET-OC) (see Table 5). For aquatic remote sensing at visible wavelengths, vicarious calibration with buoy and platform (or similar asset) is only done to address transfer-to-orbit changes in prelaunch calibration or to refine prelaunch calibration to aquatic target uncertainties and address biases in surface radiometry stemming from the atmospheric correction (Antoine et al., 2007; Clark et al., 1997; Clark et al., 2002; Vansteenwegen et al., 2019; Zibordi et al., 2009).

Table 5

Global Instrumented Aquatic Sites for Vicarious Calibration

| Site name | Location |
|---------------------|----------------------|
| Aqua Alta | 45.3142°N, 12.5083°E |
| Bahia Blanca | 39.148°S, 61.722°W |
| Casablanca Platform | 40.717°N, 1.358°E |
| Chesapeake Bay | 39.124°N, 76.349°W |
| Galata Platform | 43.045°N, 28.193°E |
| Kemigawa Offshore | 35.611°N, 140.023°E |
| Lake Okeechobee N | 27.139°N, 80.789°W |
| Lake Tahoe | 39.0°N, 120.0°W |
| LISCO | 40.955°N, 73.342°W |
| Lucinda | 18.520°S, 146.386°E |

| | |
|--------------------|-------------------------|
| Oostende | 14.7833°N, 2.9194°E |
| Palgrunden | 58.755°N, 13.152°E |
| Salton Sea | 33.22532°N, 115.82425°W |
| San Marco Platform | 2.942°S, 40.215°E |
| Section-7 Platform | 44.546°N, 29.447°E |
| Socheongcho | 37.423°N, 124.738°E |
| USC SeaPRISM | 33.564°N, 118.118°W |
| Venise | 45.314°N, 12.508°E |
| WaveCIS Site CSI 6 | 28.867°N, 90.483°W |
| Zeebrugge-MOW1 | 51.362°N, 3.120°E |
| MOBY 272 | 20.4322°N, 157.0936°W |
| BOUSSOLE | 43.367°N, 7.900°E |
| MarONet | TBD Near Perth |
| EURYBIA | TBD Mediterranean Sea |

MOBY (<https://coastwatch.noaa.gov/cw/field-observations/MOBY.html>) is a primary radiometry resource used for validation and vicarious calibration of ocean color sensors since the launch of NASA's Sea-viewing Wide Field-of-view Sensor (SeaWiFS). MOBY is moored off the island of Lanai, Hawai'i and is an autonomous optical buoy measuring daily near real time upwelling radiance (L_u) from 340-955 nm at approximately 1, 5, and 9 m depth and downwelling irradiance (E_d) from underwater at these depths and at the surface. MOBY has been in continuous operation since 1997. Progress is underway to augment MOBY with MOBY-like enhanced technology buoy systems for global coverage and to support system vicarious calibration (SVC). Additional planned sites include MarONet at the Australian site off the coast of Perth and the European Radiometry Buoy and Infrastructure (EURYBIA) for the Copernicus site near Lampedusa Island in the Mediterranean Sea (Liberti et al., 2020). SVC is required for surface radiometry for aquatic targets and accounts for instrument and other effects in atmospheric correction.

The BOUSSOLE buoy (<http://www.obs-vlfr.fr/Boussole/html/project/introduction.php>) is deployed in the Ligurian Sea (Mediterranean Sea) off of Nice, France. Radiometer measurements of irradiance are made at 4.5 m above the water surface (E_s) and downwelling irradiance, upwelling irradiance (E_u), and upwelling radiance are made at 4 and 9 m depths. Data are collected every 15 min during daylight and hourly at night. There were operational sequences of data collection beginning in 2002 and nearly uninterrupted data collections since 2005.

WATERHYPERNET (<https://waterhypernet.org/>) is a hyperspectral radiometer system (350-900 nm) network that has had prototypes deployed on a platform in the Adriatic Sea since 2018 and operating autonomously since 2019. There are three sites operating the system on platforms in Belgium: Aqua Alta, Oostende, and Blankart. Production level systems are planned for deployment at coastal and inland water sites. Downwelling irradiance, downwelling sky radiance (L_d) and upwelling radiance measurements are made with the radiometer. SBG will be working to extend this network into the USA to build calibration/validation infrastructure for the mission. This expansion will likely also include LANDHYPERNET deployments of instrument, which is a terrestrial version of the WATERHYPERNET program.

AERONET-OC (https://aeronet.gsfc.nasa.gov/new_web/ocean_color.html) is a network of identical above water multispectral radiometer measurement systems (SeaPRISM) on fixed platforms augmenting the globally distributed network of sun photometers of AERONET. There have been 38 systems installed (or moved) globally since the initial installations in 2009 and 15 of these serviced systems are operating. The SeaPRISM measures Sun irradiance, sky radiance (L_s), and total radiance from the sea (L_T) every 30 s at ocean color algorithm channels from 400 to 1020 nm. The system is designed not to collect data when clouds are obscuring the Sun. Derived normalized water-leaving radiance of the site-specific seawater apparent water properties are provided.

6 Summary

In this paper, we considered high-level calibration and validation concepts that are relevant to the SBG mission formulation and we expect that these concepts will be built on the recommendations outlined in this paper. In general, the SBG project should work with all collaborating agencies to use common metrological and radiometric language with terms derived from international standards and use common techniques for prelaunch characterization and

calibration; use and share reference sources; use common match-up datasets, reference data sets, calibration and validation methods; and use open, standard algorithms for on-orbit calibration and validation and generation of at-sensor and surface radiometry. In particular, the current recommended data set for solar spectral irradiance is the TSIS-1 Hybrid Solar Reference Spectrum (Coddington et al., 2020) for solar calibration and generation of all reflectance data products.

SBG should keep as much information and steps in common as possible in support of a suite of standard data products across missions. To that end, it is further recommended that all collaborating space agencies have advanced discussions and agreements regarding work-flows, modes of communication and conflict resolution necessary for effective collaboration towards these common resources. To support data harmonization and interoperability, the SBG CVWG recommended that this includes transformation of data onto common spatial and spectral grids and the use of ISO data standard or CEOS protocols for development of ARD. It is also recommended that a calibration and validation infrastructure be established, including the development of computational infrastructure and open-source analysis tools for comparing SBG imaging spectroscopy or thermal infrared imagery with data sets from other surface, airborne, or spaceborne sensors, as provided by collaborating agencies.

Orbital simulations for SBG VSWIR and TIR instruments reveal that orbital altitude, imaging revisit frequencies, imaging swath width of existing and planned space architectures for Earth imaging clearly underscore the need for more synergistic cooperation around designed SNO or NSO opportunities to maximize cross-mission capabilities if inter-calibration is a strategic mission priority. In addition, there are clear geographic imaging patterns for SNO and NSO that may not align very well with the established ground-based radiometric calibration reference sites. The SBG CVWG recommends better mission cooperation between US and international space agencies to optimize orbits in support of inter-calibration and higher quality terrestrial remote sensing science and application data products.

For on-orbit long-term monitoring and time-dependent, inter-calibration, Lunar calibration is recommended because only the Moon could be used as a common calibration reference free of effects from the Earth's atmosphere. But use of the Moon depends on the removal of current biases in lunar spectral irradiance predictions. A mission concept should plan on lunar observations dense in commissioning, then each month for at least a year, then becoming spaced out; also, soon after any traumatic event on the spacecraft. This includes any provisions that must be made in spacecraft design, accurate pointing and pointing knowledge, accurate and detailed knowledge of the instrument spatial response, instrument temperature control, and mission concept of operations (CONOPS). However, using solar calibration is also highly recommended to provide continuous monitoring throughout the mission, especially if the instrument design includes multiple detectors for the same band.

Validation determines whether threshold uncertainty targets are actually being met by comparing SBG satellite data products against measurements made *in situ*. The validation strategy must develop a surface sampling strategy that addresses temporal and spatial variability of the geophysical property being vetted against actual surface measurements. However, it would be ideal for the *in situ* measurement uncertainty (or some aggregate) to be less than the quality threshold uncertainty to get a meaningful result, which implies the level of quality of

measurements sought by a given validation strategy. In general, the SBG CVWG recommends that the NASA SBG project and collaborating agencies should define methods and protocols for selecting and archiving validation and vicarious calibration match-ups between *in situ* and satellite measurements.

To facilitate this development, input will be needed from the algorithm and application developers regarding the expected value, valid range, and spatial and temporal variation for each geophysical quantity identified to be produced by the SBG mission, especially any standard data products across agencies. Spatial and temporal variability must be quantified at global, scene and subpixel scales. Observing System Simulation Experiments (OSSE) results may also help to fill in knowledge gaps in the information provided by the community or literature.

The SBG CVWG also noted that future calibration and validation plans should get additional input from the algorithm and application communities regarding resources available to acquire *in situ* data, e.g., measurement networks; observation stations, towers, and buoys; airborne campaigns, cruises, and field campaigns, including efforts employing unmanned vehicles. Any SBG validation plan should draw on any existing validation protocols or studies undertaken by algorithm developers or end users in these communities, or protocols and standards accepted by international working groups. Processing infrastructure common to both validation and vicarious calibration includes, but is not limited to, ground processing software for extracting matching satellite data and capability to process surface data.

The SBG CVWG recommends that the NASA SBG project and its collaborating agencies identify or develop joint surface measurement networks. Instrumented terrestrial and aquatic networks of sites for radiometric, thermal, spectral, and geometric calibration are critical to the generation of high-quality science data products. Likewise, arrays of surface instruments are necessary for collection of a large sample of validation data. This paper has touched on a sizable sample of potential resources; however, it remains unclear what portion of existing resources will be available later in this decade when the SBG mission is in orbit. The project will need to track these resources and perhaps even be prepared to support their maintenance to assure adequate surface data is available for calibration, validation and algorithm development.

References

Alonso, K., Bachmann, M., Burch, K., Carmona, E., Cerra, D., De los Reyes, R., Dietrich, D., Heiden, U., Hölderlin, A., Ickes, J. and Knodt, U., Krutz, D., Lester, H., Müller, R., Pagnutti, M., Reinartz, P., Richter, R., Ryan, R., Sebastian, I., & Tegler, M. (2019). Data products, quality and validation of the DLR Earth sensing imaging spectrometer (DESI). *Sensors*, 19(20), 4471. doi:10.3390/s19204471

Anderson, G. P., Berk, A., Acharya, P. K., Matthew, M. W., Bernstein, L.S., Chetwynd Jr., J. H., Dothe, H., Adler-Golden, S. M., Ratkowski, A. J., Felde, G.W., Gardner, J. A., Hoke, R. L., Richtsmeier, S. C., Pukall, B., Mello, J. B. & Jeong, L. S. (2000). MODTRAN4: radiative transfer modeling for remote sensing. *Proc. SPIE*, 4049:176-183. doi:10.1117/12.410338

Antoine, D., Guevel, P., Deste, J.-F., Becu, G., Louis, F., Scott, A. J., & Bardey, P. (2008). The “BOUSSOLE” Buoy—A New Transparent-to-Swell Taut Mooring Dedicated to Marine Optics:

Design, Tests, and Performance at Sea. *Journal of Atmospheric and Oceanic Technology*, 25, 968-989. doi: 10.1175/2007JTECHO563.1

Barnsley, M., Settle, J., Cutter, M., Lobb, D., & Teston, F. (2004). The PROBA/CHRIS mission: A low-cost smallsat for hyperspectral multiangle observations of the Earth surface and atmosphere. *IEEE Trans. Geosci. Remote Sens.* 42, 1512–1520.
<https://doi.org/10.1109/TGRS.2004.827260>

Bilimoria, K. D. & Krieger, R. A. (2011). Slot Architecture for Separating Satellites in Sun-Synchronous Orbits. AIAA SPACE 2011 Conference & Exposition.

BIPM, I., IFCC, I., ISO, I., & IUPAP, O. (2008). Evaluation of Measurement Data-Guide to the Expression of Uncertainty in Measurement (GUM 1995 with minor corrections). Joint Committee for Guides in Metrology, JCGM, 100.

Brell, M., Guanter, L., Segl, K., Scheffler, D., Bohn, N., Bracher, A., Soppa, M.A., Foerster, S., Storch, T., Bachmann, M. & Chabrillat, S. (2021). The EnMAP Satellite–Data Product Validation Activities. In *2021 11th Workshop on Hyperspectral Imaging and Signal Processing: Evolution in Remote Sensing (WHISPERS)* (pp. 1-5). IEEE.
doi:10.1109/WHISPERS52202.2021.9484000

Bouvet, M., Thome, K., Berthelot, B., Bialek, A., Czapla-Myers, J., Fox, N. P., Goryl, P., Henry, P., Ma, L., Marcq, S., Meygret, A., Wenny, B. N., & Woolliams, E. R. (2019). RadCalNet: A Radiometric Calibration Network for Earth Observing Imagers Operating in the Visible to Shortwave Infrared Spectral Range. *Remote Sens.*, 11, 2401. doi:10.3390/rs11202401

Cao, C. and A. K. Heidinger. 2002: Intercomparison of the longwave infrared channels of MODIS and AVHRR/NOAA-16 using simultaneous nadir observations at orbit intersections. In *Earth Observing Systems VII*, William L. Barnes (editor), Proceedings of SPIE, 4814:306-316.

Cao, C., Weinreb, M., & Xu, H. (2004). Predicting simultaneous nadir overpasses among polar-orbiting meteorological satellites for the intersatellite calibration of radiometers. *Journal of Atmospheric and Oceanic Technology*, 21(4), 537-542.

Cao, C., C., H. Xu, J. Sullivan, L. Mcmillin, P. Ciren, and Y. Hou, 2005: Intersatellite radiance biases for the High Resolution Infrared Radiation Sounders (HIRS) on-board NOAA-15, -16, and -17 from simultaneous nadir observations. *J. Atmos. and Ocn. Tech.*, 22, 381-395.

Chapman, J. W., Thompson, D. R., Helmlinger, M. C., Bue, B. D., Green, R. O., Eastwood, M.L., Geier, S., Olson-Duvall, W., & Lundeen, S. R. (2019). Spectral and radiometric calibration of the next generation airborne visible infrared spectrometer (AVIRIS-NG). *Remote Sensing*, 11(18), 2129. doi: 10.3390/rs11182129

- Choi, T., Xiong, X. & Wang, Z. (2014). On-Orbit Lunar Modulation Transfer Function Measurements for the Moderate Resolution Imaging Spectroradiometer, *IEEE Transactions on Geoscience and Remote Sensing*, 52(1), 270-277, doi: 10.1109/TGRS.2013.2238545
- Clark, D. K., Gordon, H. R., Voss, K. J., Ge, Y., Broenkow, W., & Trees C. (1997). Validation of atmospheric correction over the oceans. *Journal of Geophysical Research: Atmospheres*, 102(D14), 17209-17217. doi: 10.1029/96JD03345
- Clark, D. K., Yarbrough, M. A., Feinholz, M. E., Flora, S., Broenkow, W., Kim, Y. S., Johnson, B. C., Brown, S. W., Yuen, M., & Mueller, J. L. (2002). MOBY, a radiometric buoy for performance monitoring and vicarious calibration of satellite ocean color sensors: Measurement and data analysis protocols. *Ocean Optics Protocols for Satellite Ocean Color Sensor Validation, Revision 3, Volume 2*. J. L. Mueller and G. S. Fargion, Eds. Greenbelt, MD, NASA Goddard Space Flight Center. NASA/TM--2002-21004:138-170.
- Clark, R. N., Swayze, G. A., Livo, K. E., Kokaly, R. F., King, T. V., Dalton, J. B., Vance, J. S., Rockwell, B. W., Hoefen, T. M., & McDougal, R. R. (2002). Surface reflectance calibration of terrestrial imaging spectroscopy data: a tutorial using AVIRIS. In *Proceedings of the 10th Airborne Earth Science Workshop* (Vol. 2). Pasadena, CA, USA: Jet Propulsion Laboratory.
- Clerc, S., Van Malle, M. N., Massera, S., Quang, C., Chambrelan, A., Guyot, F., Pessiot, L., Iannone, R. & Boccia V. (2021). Copernicus SENTINEL-2 Geometric Calibration Status, *IEEE International Geoscience and Remote Sensing Symposium*, pp. 8170-8172, doi: 10.1109/IGARSS47720.2021.9555090
- Cocks, T., Jenssen, R., Stewart, A., Wilson, I., and Shields, T., 1998, The HyMap airborne hyperspectral sensor: The system, calibration and performance: European Association of Remote Sensing Laboratories (EARSeL) Workshop on Imaging Spectroscopy, Zurich, October 6–8, 1998, Extended Abstracts, p. 37–43.
- Coddington, O. M., Richard, E. C., Harber, D., Pilewskie, P., Woods, T. N., Chance, K., et al. (2021). The TSIS-1 Hybrid Solar Reference Spectrum. *Geophysical Research Letters*, 48, e2020GL091709. <https://doi.org/10.1029/2020GL091709>
- Coddington, O., Lean, J., Pilewskie, P., Snow, M., Richard, E., Kopp, G., et al. (2019). Solar Irradiance variability: comparisons of models and measurements. *Earth and Space Science*, 6, 2525-2555. <https://doi.org/10.1029/2019EA000693>
- Coll, C., Z. Wan, & Galve, J. M. (2009), Temperature-based and radiance-based validations of the V5 MODIS land surface temperature product, *J. Geophys. Res.*, 114, D20102, doi:10.1029/2009JD012038.
- Coppo, P., Taiti, A., Pettinato, L., Francois, M., Taccola, M., & Drusch, M. (2017). Fluorescence imaging spectrometer (FLORIS) for ESA FLEX mission. *Remote Sensing*, 9(7), 649. doi: 10.3390/rs9070649

Cosnefroy, H., Leroy, M., & Briottet, X., (1996). Selection and Characterization of Saharan and Arabian Desert Sites for the Calibration of Optical Satellite Sensors. *Remote Sensing of Environment*, 58(1), 101-114. [doi:10.1016/0034-4257\(95\)00211-1](https://doi.org/10.1016/0034-4257(95)00211-1)

Czajkowski, K. P., Goward, S. N., Stadler, S. J. & Walz, A. (2000). Thermal Remote Sensing of Near Surface Environmental Variables: Application Over the Oklahoma Mesonet, *The Professional Geographer*, 52(2), 345-357. doi:10.1111/0033-0124.00230

Czapla-Myers, J., Thome, K., Wenny, B., & Anderson, N. (2020). Railroad Valley Radiometric Calibration Test Site (RadCaTS) as Part of a Global Radiometric Calibration Network (RadCalNet)," *IGARSS 2020 - 2020 IEEE International Geoscience and Remote Sensing Symposium, 2020*, pp. 6413-6416, doi:10.1109/IGARSS39084.2020.9323665

Datla, R. U., Rice, J. P., Lykke, K. R., Johnson, B. C., Butler, J. J. & Xiong, X. (2011). Best practice guidelines for pre-launch characterization and calibration of instruments for passive optical remote sensing. *Journal of Research of the National Institute of Standards and Technology*, 116(2), 621. doi: 10.6028/jres.116.009

Dechoz, C., Poulain, V., Massera, S., Languille, F., Greslou, D., de Lussy, F., Gaudel, A., L'Helguen, C., Picard, C., & Trémas, T. (2015). Sentinel 2 global reference image. *Image and Signal Processing for Remote Sensing XXI*. Proc. SPIE, 9643, 96430A. doi: 10.1117/12.2195046

Dollfus, A. (1962). The Polarization of Moonlight. In Z. Kopal and K. Mikhailov (Eds.), *Physics and Astronomy of the Moon* (pp. 131-159). New York and London: Academic Press.

Durell, C. (2019). IEEE P4001 Hyperspectral Standard: Progress and Cooperation. *IGARSS 2019 - 2019 IEEE International Geoscience and Remote Sensing Symposium*, 4432-4434. doi: 10.1109/IGARSS.2019.8900295

Durell, C., & Russell, B. (2020). Durell On Demand Vicarious Calibration for Analysis Ready Data: The FLARE Network, Proceedings of 34th Annual Small Satellite Conference. SSC20-S1-01.

Feingersh, T., & Dor, E. B. (2015). SHALOM—A commercial hyperspectral space mission. In Shen-En Qian (Ed.), *Optical payloads for space missions* (pp. 247-262). doi:10.1002/9781118945179.ch11

Ferrero, C. (2009). Vocabulaire international des termes fondamentaux et généraux de métrologie (VIM). Presented at Istituto Nazionale di Ricerca Metrologica (INRIM), Tunis, Tunisia. doi:10.13140/RG.2.1.3771.4320

Green, R. O., Pavri, B. E., & Chrien, T. G. (2003). On-orbit radiometric and spectral calibration characteristics of EO-1 Hyperion derived with an underflight of AVIRIS and in situ measurements at Salar de Arizaro, Argentina. *IEEE Transactions on Geoscience and Remote Sensing*, 41(6), 1194-1203. doi: 10.1109/TGRS.2003.813204

Green, R. O., Mahowald, N., Ung, C., Thompson, D. R., Bator, L., Bennet, M., et al. (2020). The Earth surface mineral dust source investigation: An Earth science imaging spectroscopy mission. In *2020 IEEE Aerospace Conference* (pp. 1-15). IEEE. doi: 10.1109/AERO47225.2020.9172731

Guanter, L., Kaufmann, H., Segl, K., Foerster, S., Rogass, C., Chabrillat, S., et al. (2015). The EnMAP spaceborne imaging spectroscopy mission for earth observation. *Remote Sensing*, 7(7), 8830-8857. doi: 10.3390/rs70708830

Guillevic, P., Göttsche, F., Nickeson, J., Hulley, G., Ghent, D., Yu, Y., Trigo, I., Hook, S., Sobrino, J.A., Remedios, J., Román, M. & Camacho, F. (2018). Land Surface Temperature Product Validation Best Practice Protocol. Version 1.1. In P. Guillevic, F. Göttsche, J. Nickeson & M. Román (Eds.), *Good Practices for Satellite-Derived Land Product Validation* (p. 58): Land Product Validation Subgroup (WGCV/CEOS), doi:10.5067/doc/ceoswgcv/lpv/lst.001

Gutman, G., Huang, C. & Chander, G. (2013). Assessment of the NASA-USGS Global Land Survey (GLS) datasets. *Remote Sens. Environ.*, 134, 249–265.

Hall, D.K., Box, J.E., Casey, K.A., Hook, S.J., Shuman, C.A. & Steffen, K. (2008). Comparison of satellite-derived and in-situ observations of ice and snow surface temperatures over Greenland. *Remote Sensing of Environment*, 112(10), 3739-3749, doi:10.1016/j.rse.2008.05.007

Helder, D., Thome, K.J., Mishra, N., Chander, G., Xiong, X., Angal, A., & Choi, T. (2013). Absolute Radiometric Calibration of Landsat Using a Pseudo Invariant Calibration Site. *IEEE Transactions on Geoscience and Remote Sensing*, 51(3), 1360-1369. doi: 10.1109/TGRS.2013.2243738

Holben B.N., Eck, T.F., Slutsker, I., Tanre, D., Buis, J.P., Setzer, A., Vermote, E., Reagan, J.A., Kaufman, Y., Nakajima, T., Lavenu, F., Jankowiak, I., & Smirnov, A.. (1998). AERONET - A federated instrument network and data archive for aerosol characterization, *Remote Sensing of Environment*, 66, 1-16.

Hook, S., Cawse-Nicholson, K., Barsi, J., Radocinski, R., Hulley, G., Johnson, W., Rivera, G., & Markham, B. (2020). In-Flight Validation of the ECOSTRESS, Landsats 7 and 8 Thermal Infrared Spectral Channels Using the Lake Tahoe CA/NV and Salton Sea CA Automated Validation Sites. *IEEE Transactions on Geoscience Remote Sensing*, 58(2), 1294-1302. doi:10.1109/TGRS.2019.2945701

Hook, S. J., Vaughan, R. G., Tonooka, H. & Schladow S. G. (2007). Absolute Radiometric In-Flight Validation of Mid Infrared and Thermal Infrared Data from ASTER and MODIS on the Terra Spacecraft Using the Lake Tahoe, CA/NV, USA, Automated Validation Site. *IEEE Transactions on Geoscience and Remote Sensing*, 45(6), 1798-1807. doi:10.1109/TGRS.2007.894564

Iwasaki, A., Ohgi, N., Tanii, J., Kawashima, T., & Inada, H. (2011). Hyperspectral Imager Suite (HISUI)-Japanese hyper-multi spectral radiometer. In *2011 IEEE International Geoscience and Remote Sensing Symposium* (pp. 1025-1028). IEEE. doi: 10.1109/IGARSS.2011.6049308

Khakurel, P., Leigh, L., Kaewmanee, M., & Teixeira Pinto, C. (2021). Extended Pseudo Invariant Calibration Site-Based Trend-to-Trend Cross-Calibration of Optical Satellite Sensors. *Remote Sensing*, 13(8). 1545. [doi:10.3390/rs13081545](https://doi.org/10.3390/rs13081545)

Kieffer, H. H. (1997). Photometric stability of the lunar surface. *Icarus*, 130, 323–327.

Kieffer, H. (2021a). Advances in the SLIM lunar spectral irradiance model: Many observations, one Moon. In *CALCON 2021 Proceedings, Logan, UT. Conference on Characterization and Calibration for Remote Sensing*.
<https://digitalcommons.usu.edu/calcon/CALCON2021/all2021content/23>

Kieffer, H. (2021b). Status of the SLIMED model; converging on the real Moon. In *GSICS VIS/NIR Web Meeting for August 2021. Global Space-based Inter-Calibration System*.
http://gsics.atmos.umd.edu/pub/Development/20210812/Kieffer_21octGVN.pdf

Kieffer, H. (2022). Multiple instrument based spectral irradiance of the Moon (2022). *J. Ap. Remote Sensing*,. Vol. 16, Issue 3

<https://doi.org/10.1117/1.JRS.16.038502>

Kieffer, H. H., Mullins, K. F., & MacKinnon, D. J., (2008). Validation of the ASTER instrument Level 1A scene geometry. *Photogrammetric Engineering & Remote Sensing*, 74(3), 289-301. doi:10.14358/PERS.74.3.289. [Data files available from USGS EROS]

Kieffer, H. H. & Stone, T. C. (2005). The spectral irradiance of the Moon. *Astron. Jour.*, 129, 2887–2901.

Knight, E. & Kvaran, G. (2014). Landsat-8 Operational Land Imager design, characterization and performance, *Remote Sens.*, 6(11), 10286-10305. <https://doi.org/10.3390/rs61110286>

Krutz, D., Müller, R., Knodt, U., Günther, B., Walter, I., Sebastian, I., Säuberlich, T., Reulke, R., Carmona, E., Eckardt, A., Venus, H., Fischer, C., Zender, B., Arloth, S., Lieder, M., Neidhardt, M., Grote, U., Schrandt, F., Gelmi, S., & Wojtkowiak, A. (2019). The instrument design of the DLR earth sensing imaging spectrometer (DESI). *Sensors*, 19(7), 1622. doi: 10.3390/s19071622

Lean, J. L., Coddington, O., Marchenko, S. V., Machol, J., DeLand, M. T., & Kopp, G. (2020). Solar irradiance variability: Modeling the measurements. *Earth and Space Science*, 7, e2019EA000645. <https://doi.org/10.1029/2019EA000645>

Li, X., Wu, T., Liu, K., Li, Y., & Zhang, L. (2016). Evaluation of the Chinese fine spatial resolution hyperspectral satellite TianGong-1 in urban land-cover classification. *Remote Sensing*, 8(5), 438. doi: 10.3390/rs8050438

- Liberti, G.L., D'Alimonte, D., di Sarra, A., Mazeran, C., Voss, K., Yarbrough, M., Bozzano, R., Cavaleri, L., Colella, S., Cesarini, C., Kajiyama, T., Meloni, D., Pomaro, A., Volpe, G., Yang, C., Zagolski, F., & Santoleri, R. (2020). European Radiometry Buoy and Infrastructure (EURYBIA): A Contribution to the Design of the European Copernicus Infrastructure for Ocean Colour System Vicarious Calibration. *Remote Sensing*, 12(7)1178. doi:10.3390/rs12071178
- Lin, G., Wolfe, R.E., Dellomo, J. J., Tan, B. & Zhang, P. (2020). SNPP and NOAA-20 VIIRS on-orbit geolocation trending and improvements. *Earth Observing Systems XXV*, edited by J. J. Butler, X. Xiong, X. Gu, Proc. SPIE Vol. 11501, 1150112, doi: 10.1117/12.2569148
- Lin, G., Wolfe, R. E. & Nishihama, M. (2011). NPP VIIRS Geometric Performance Status, *Earth Observing Systems XVI*, edited by J. J. Butler, X. Xiong, X. Gu, Proc. of SPIE, Vol. 8153, 81531V, doi: 10.1117/12.894652
- Lin, G., Wolfe, R. E. & Tilton, J. C. (2016). Trending of SNPP ephemeris and its implications on VIIRS geometric performance. *Earth Observing Systems XXI*, edited by J. J. Butler, X. Xiong, X. Gu, Proc. of SPIE Vol. 9972, 99721K, doi: 10.1117/12.2239043
- Lin, G., Wolfe, R. E., Tilton, J. C., Zhang, P., Dellomo, J. J., & B. Tan, T. (2018). JPSS-1/NOAA-20 VIIRS early on-orbit geometric performance. *Earth Observing Systems XXIII*, edited by J. J. Butler, X. Xiong, X. Gu, Proc. SPIE 10764, 107641H, doi: 10.1117/12.2320767
- Lin, G., Wolfe, R. E., Zhang, P., Tilton, J. C., Dellomo, J. J. & Tan, B. (2019). Thirty-six combined years of MODIS geolocation trending. *Earth Observing Systems XXIV*, edited by J. J. Butler, X. Xiong, X. Gu, Proc. SPIE Vol. 11127, 1112715, doi: 10.1117/12.2529447
- Maiersperger, T. K., Scaramuzza, P. L., Leigh, L., Shrestha, S., Gallo, K. P., Jenkerson, C. B., & Dwyer, J. L. (2013). Characterizing LEDAPS surface reflectance products by comparisons with AERONET, field spectrometer, and MODIS data. *Remote Sensing of Environment*, 136, 1-13. doi: 10.1016/j.rse.2013.04.007
- Malthus, T. J., Ong, C., Lau, I., Fearn, P., Byrne, G., Thankappan, M., Chisholm, L., Suarez, L., Clarke, K., Scarth, P. & Phinn, S. (2019). A Community Approach to the Standardised Validation of Surface Reflectance Data. *A Technical Handbook to Support the Collection of Field Reflectance Data. Release version 2.0*, January 2019. CSIRO, Australia. ISBN: 978-1-4863-0991-7

Masek, J. G., Wulder, M. A., Markham, B., McCorkel, J., Crawford, C. J., Storey, J., & Jenstrom, D. T. (2020). Landsat 9: Empowering open science and applications through continuity. *Remote Sensing of Environment*, 248, 111968. doi: 10.1016/j.rse.2020.111968

Micijevic, E., Rengarajan, R., Haque, M.O., Lubke, M., Tuli, F.T.Z., Shaw, J.L., Hasan, N., Denevan, A., Franks, S., Choate, M.J., Anderson, C., Markham, B., Thome, K., Kaita, E., Barsi, J., Levy, R., and Ong, L., 2022, ECCOE Landsat quarterly Calibration and Validation report—Quarter 3, 2021: U.S. Geological Survey Open-File Report 2022–1025, 38 p., doi: 10.3133/ofr20221025

Müller, R. (2014). Calibration and verification of remote sensing instruments and observations. *Remote Sensing*, 6(6), 5692-5695. doi: 10.3390/rs6065692

National Academies of Sciences, Engineering, and Medicine. (2018). *Thriving on Our Changing Planet: A Decadal Strategy for Earth Observation from Space*. Washington, DC: The National Academies Press. doi:10.17226/24938

National Oceanic and Atmospheric Administration, Earth System Research Laboratory, 1995: Surface Radiation Budget (SURFRAD) Network Observations. NOAA National Centers for Environmental Information.

Nicodemus, F. E., Richmond, J. C., Hsia, J. J., Ginsberg, I. W., & Limperis, T. (1977). Geometrical considerations and nomenclature for reflectance. Final Report National Bureau of Standards.

Ong, C., Thome, K., Heiden, U., Czapla-Myers, J., & Mueller, A. (2018). Reflectance-Based Imaging Spectrometer Error Budget Field Practicum at the Railroad Valley Test Site, Nevada [Technical Committees]. *IEEE Geoscience and Remote Sensing Magazine*, 6(3), 111-115. doi: 10.1109/MGRS.2018.2841934

Pearlshtien, D. H., Pignatti, S., Greisman-Ran, U., & Ben-Dor, E. (2021). PRISMA sensor evaluation: a case study of mineral mapping performance over Makhtesh Ramon, Israel. *International Journal of Remote Sensing*, 42(15), 5882-5914. doi: 10.1080/01431161.2021.1931541

Pearlshtien, D. H., & Ben-Dor, E. (2022). Calval Evaluation of Desis Products in Amiaz Plain and Makhtesh Ramon Test Sites, Southern Israel. *The International Archives of Photogrammetry, Remote Sensing and Spatial Information Sciences*, 46, 13-21.

Pérez Díaz, C.L., Xiong, X., Li, Y., & Chiang, K. (2021). S-NPP VIIRS Thermal Emissive Bands 10-Year On-Orbit Calibration and Performance. *Remote Sensing*, 13(19), 3917. doi:10.3390/rs13193917

Pignatti, S., Palombo, A., Pascucci, S., Romano, F., Santini, F., Simoniello, T., Umberto, A., Vincenzo, C., Acito, N., Diani, M., & Ananasso, C. (2013, July). The PRISMA hyperspectral mission: Science activities and opportunities for agriculture and land monitoring. In *2013 IEEE International Geoscience and Remote Sensing Symposium-IGARSS* (pp. 4558-4561). IEEE. doi: 10.1109/IGARSS.2013.6723850

Polz, L., Serdyuchenko, A., Lettner, M., Mücke, M., & Fischer, S. (2020). Setups for alignment and on-ground calibration and characterization of the EnMAP hyperspectral imager. *Proceedings of SPIE 11852, International Conference on Space Optics — ICSO 2020*, 118526B. doi:10.1117/12.2600240

Quattrochi, D.A., & Luvall, J.C. (Eds.). (2004). *Thermal Remote Sensing in Land Surface Processes*. Boca Raton, Florida. Taylor & Francis Group, CRC Press LLC.

Rengarajan, R., Sampath, A., Storey, J., & Choate, M. (2015). Validation of Geometric Accuracy of Global Land Survey (GLS) 2000 Data. *Photogrammetric Engineering and Remote Sensing*, 81(2),131-141. doi:10.14358/PERS.81.2.131

Rengarajan, R.; Storey, J.C.; Choate, M.J. (2020). Harmonizing the Landsat Ground Reference with the Sentinel-2 Global Reference Image Using Space-Based Bundle Adjustment, *Remote Sens.*, 12(19), 2132, <https://doi.org/10.3390/rs12193132>

Richter, R., & Schläpfer, D. (2019). Atmospheric and topographic correction (ATCOR theoretical background document) Version 1.1, March 2021. DLR Report DLR-IB 564-03/2019; German Aerospace Center (DLR): Wessling, Germany, 2019; Available online: https://www.rese-apps.com/pdf/atcor_atbd.pdf (accessed on 29 March 2022).

Schaepman-Strub, G., Schaepman, M.E., Painter, T.H., Dangel, S., Martonchik, J.V. (2006). Reflectance quantities in optical remote sensing—definitions and case studies, *Remote Sensing of Environment*, 103(1), 27-42. doi:10.1016/j.rse.2006.03.002

Seo, D., Oh, J., Lee, C., Lee, D. & Choi, H. (2016). Geometric Calibration and Validation of Kompsat-3A AEISS-A Camera, *Sensors*, 16(10), 1776. doi:10.3390/s16101776

Stavros, E. N., Jon Chrone, J., Cawse-Nicholson, K., Freeman, A., Glenn, N. F., Guild, L., Kokaly, R., Lee, C., Luvall, J., Pavlick, R., Poulter, B., Schollaert Uz, S., Serbin, S., Thompson, D. R., Townsend, P.A., Turpie, K., Yuen, K., Thome, K., Wang, W., Zareh, S.-K., Nastal, J., Bearden, D., Miller, C. E., Schimel, D. (2022). Designing an Observing System to Study the Surface Biology and Geology of the Earth in the 2020s. *Journal of Geophysical Research - Biogeoscience*. doi:10.1002/essoar.10509039.1

Stone, T.C., Coddington, O., Bak, J., Doelling, D. (2021), Vis/NIR subgroup proposes TSIS-1 HRSR as the GSICS recommended solar spectrum, GSICS Quarterly Newsletter Spring 2021 Issue, 15(1). Editor: Ball, M. doi: 10.25923/m6pq-w122

Stone, T. C., Kieffer, H. H., Lukashin, C., & Turpie, K. (2020). The Moon as a Climate-quality Radiometric Calibration Reference. 12:1837. doi:10.3390/rs12111837

Storch, T., Bachmann, M., Honold, H. P., Kaufmann, H., Krawczyk, H., Müller, R., Sang, B., Schneider, M., Segl, K. & Chlebek, C. (2014, July). EnMAP data product standards. In *2014 IEEE Geoscience and Remote Sensing Symposium* (pp. 2586-2589). IEEE. doi: 10.1109/IGARSS.2014.6947002

- Storey, J.C., Choate, M. & Lee, K. (2014). Landsat 8 Operational Land Imager On-Orbit Geometric Calibration and Performance, *Remote Sensing*, 6(11), 11127–11152. doi:10.3390/rs6111127
- Storey, J.C.; Rengarajan, R.; Choate, M.J. (2019). Bundle Adjustment Using Space-Based Triangulation Method for Improving the Landsat Global Ground Reference. *Remote Sensing*, 11(14), 1640; <https://doi.org/10.3390/rs11141640>
- Sun, J. & Xiong, X. (2021). Improved Lunar Irradiance Model Using Multiyear MODIS Lunar Observations. *IEEE Transactions on Geoscience and Remote Sensing*, 59(6):5154–5170. doi:10.1109/TGRS.2020.3011831
- Swayze, G. A., Clark, R. N., Goetz, A. F., Livo, K. E., Breit, G. N., Kruse, F. A., ... & Ashley, R. P. (2014). Mapping advanced argillic alteration at Cuprite, Nevada, using imaging spectroscopy. *Economic geology*, 109(5), 1179-1221. doi: 10.2113/econgeo.109.5.1179
- Tansock, J., Bancroft, D., Butler, J. Cao, C., Datla, R., Hansen, S., Helder, D., Kacker, R., Latvakoski, H., Mlynczak, M., Murdock, T., Peterson, J., Pollock, D., Russell, R., Scott, D., Seamons, J., Stone, T., Thurgood, A., Williams, R., Xiong, X. & Yoon, H. (2015). *Guidelines for Radiometric Calibration of Electro-Optical Instruments for Remote Sensing*, NISTHB 157. Gaithersburg, MD. doi:10.6028/NIST.HB.157
- Taylor, S., Adriaensen, S., Toledano, C., Barreto, A., Woolliams, E., & Bouvet, M. (2021). LIME: the Lunar Irradiance Model of the European Space Agency. In EGU General Assembly 2021, online, 30 Apr 2021. doi:10.5194/egusphere-egu21-10066
- Thompson, D. R., Brodrick, P. G., Cawse-Nicholson, K., Dana Chadwick, K., Green, R. O., Poulter, B., Serbin, S., Shiklomanov, A.N., Townsend, P.A., & Turpie, K.R. (2021). Spectral fidelity of Earth's terrestrial and aquatic ecosystems. *Journal of Geophysical Research: Biogeosciences*, 126(8): e2021JG006273. doi:10.1029/2021JG006273
- Tilton, J. C, Lin, G. & Tan, B. (2017b). Measurement of the Band-to-Band Registration of the SNPP VIIRS Imaging System from On-Orbit Data, *J. Selected Topics in Applied Earth Observations and Remote Sensing*, 10(3),1056-1067. doi:10.1109/JSTARS.2016.2601561
- Tilton, J. C., Wolfe, R.E. & Lin, G. (2017a). On-Orbit Line Spread Function Estimation of the SNPP VIIRS Imaging System from Lake Pontchartrain Causeway Bridge Images, *J. Selected Topics in Applied Earth Observations and Remote Sensing*, 10(11), 5056-5072. doi:10.1109/JSTARS.2017.2729879
- Tilton, J. C., Wolfe, R.E., Lin, G. & Dellomo, J.J. (2019). On-Orbit Measurement of the Effective Focal Length and Band-to-Band Registration of Satellite-Borne Whiskbroom Imaging Sensors. *Journal of Selected Topics in Applied Earth Observations and Remote Sensing*, 12(11), 4622-4633. doi:10.1109/JSTARS.2019.2949677
- USGS (2018). USGS EROS Archive - Aerial Photography - Digital Orthophoto Quadrangle (DOQs). Available online:

<https://www.usgs.gov/centers/eros/science/usgs-eros-archive-aerial-photography-digital-ortho-photo-quadrangle-doqs#overview>.

USGS (2021). Landsat 8-9 Calibration and Validation (Cal/val) Algorithm Description Document (ADD). Available online:

<https://www.usgs.gov/media/files/landsat-8-9-calibration-validation-algorithm-description-document>.

Vane, G., Goetz, A. F., & Wellman, J. B. (1984). Airborne imaging spectrometer: A new tool for remote sensing. *IEEE Transactions on Geoscience and Remote Sensing*, 6, 546-549.

Vansteenkoven, D., Ruddick, K., Cattrijsse, A., Vanhellemont, Q., & Beck, M. (2019). The pan-and-tilt hyperspectral radiometer system (PANTHYR) for autonomous satellite validation measurements – prototype design and testing. *Remote Sensing*, 11(11), 1360. doi:10.3390/rs11111360

Vuppala, H. (2017). Normalization of Pseudo-invariant Calibration Sites for Increasing the Temporal Resolution and Long-Term Trending, *Electronic Theses and Dissertations, South Dakota State University*, 2180. <https://openprairie.sdstate.edu/etd/2180>

Wan, Z., Y. Zhang, Q. Zhang, & Li, Z.-L. (2002), Validation of the land surface temperature products retrieved from Terra Moderate Resolution Imaging Spectroradiometer data. *Remote Sens. Environ.*, 83, 163-180. doi:10.1016/S0034-4257(02)00093-7.

Wang, M., Yang, B., Hu, F., & Zang, X. (2014). On-orbit geometric calibration model and its applications for high-resolution optical satellite imagery. *Remote sensing*, 6(5), 4391-4408. doi:10.3390/rs6054391

Wang, Y., Hu, X., Chen, L., Huang, Y., Li, Z., Wang, S., Zhang, P., Wu, R., Zhang, L., & Wang, W. (2020). Comparison of the Lunar Models Using the Hyper-Spectral Imager Observations in Lijiang, China. *Remote Sensing*, 12(11). doi:10.3390/rs12111878

Wang, Z., Xiong, X. and Li, Y. (2015). Update of VIIRS On-Orbit Spatial Parameters Characterized with the Moon, *IEEE Transactions on Geoscience and Remote Sensing*, 53(10), 5486-5494. doi:10.1109/TGRS.2015.2423633

Wenny, B. N., Helder, D., Hong, J., Leigh, L., Thome, K. J. & Reuter, D. (2015). Pre- and Post-Launch Spatial Quality of the Landsat 8 Thermal Infrared Sensor, *Remote Sens.*, 7, 1962-1980, doi:10.3390/rs70201962

Wilkins, L., Sang, B., Erhard, M., Bittner, H., Grzesik, A., Eberle, S., Bräuninger, C., Sornig, M., & Fischer, S. (2017, September). An on-board calibration assembly (OBCA) on the ENMAP satellite. In *International Conference on Space Optics—ICSO 2016* (Vol. 10562, p. 1056244). International Society for Optics and Photonics. doi: 10.1117/12.2296123

Xiong, X., Angal, A., Chang, T., Chiang, K., Lei, N., Li, Y., Sun, J., Twedt, K., & Wu, A. (2020). MODIS and VIIRS Calibration and Characterization in Support of Producing Long-Term High-Quality Data Products. *Remote Sensing*, 12(19), 3167. doi:10.3390/rs12193167

Xiong, X., Wenny, B.N., Wu, A., Barnes, W.L. & Salomonson, V.V. (2009). Aqua MODIS Thermal Emissive Band On-Orbit Calibration, Characterization, and Performance. *IEEE Transactions on Geoscience and Remote Sensing*, 47(3), 803-814.
doi:10.1109/TGRS.2008.2005109

Zibordi, G., Melin, F., Berthon, J.-F., Holben, B., Slutsker, I., Giles, D., D'Alimonte, D., Vandemark, D., Feng, H., Schuster, G., Fabbri, B. E., Kaitala, S., & Seppala J. (2009). AERONET-OC: A network for the validation of ocean color primary products. *Journal of Atmospheric and Oceanic Technology*, 26(8), 1634-1651. doi:10.1175/2009JTECHO654.1

Appendix A - Acronyms

AERONET, AErosol RObotic NETwork

AERONET-OC, AERONET - Ocean Color

AIS, Airborne Imaging Spectrometer

AOP, apparent optical properties

ARD, Analysis Ready Data

ASR, absolute spectral response

AVIRIS, Airborne Visible / InfraRed Imaging Spectrometer

BBR, band-to-band registration

BOUSSOLE, Buoy for the acquisition of long-term optical time series

BRDF, Bi-Directional Reflectance Distribution Function

Cal/Val, Calibration and Validation

CE90, circular error at the 90th percentile

CEOS, Committee on Earth Observation Satellites

CHIME, Copernicus Hyperspectral Imaging Mission for the Environment

CNES, Centre National d'Etudes Spatiales (The French Space Agency)

CHRIS, Compact High Resolution Imaging Spectrometer

CLARREO, Climate Absolute Radiance and Refractivity Observatory

CONOPS, concept of operations

CPF, CLARREO-Pathfinder

CVWG, Calibration and Validation Working Group (of the SBG Mission)

DEM, Digital Elevation Model

DESIS, German Aerospace Center (DLR, Deutsches Zentrum für Luft- und Raumfahrt) Earth Sensing Imaging Spectrometer

DO, Designated Observable

DOQ, digital orthophoto quadrangles

ECOSTRESS, ECOsystem Spaceborne Thermal Radiometer Experiment on Space Station

EGM, Earth Gravitational Model

EMIT, Earth Surface Mineral Dust Source Investigation

EnMAP, Environmental Mapping and Analysis Program

EOC, early orbit check-out

EPICS, extended PICS

ESA, European Space Agency

ESAS, Earth Science and Application from Space

EURYBIA, European Radiometry Buoy and Infrastructure

FLARE, Field, Line-of-sight Automated Radiance Exposure

FLEX, FLuorescence EXplorer mission

FWHM, full width at half maximum

GCP, Ground Control Point

GLS, Global Land Survey

GRI, Global Reference Image

GSD, ground sampling distance

GSICS, Global Space-based Inter-Calibration System

HISUI, Hyperspectral Imager Suite

HyMap, an airborne hyperspectral sensor, (see Cocks et al., 1998)

HYPERNETS, hyperspectral radiometer integrated in automated networks of water and land bidirectional reflectance measurements for satellite validation

HSRS, Hybrid Solar Reference Spectrum of TSIS-1

ICV, intensive calibration and validation

IFOV, instantaneous field of view

IOP, inherent optical properties

ISO, International Organization for Standardization

ISS, International Space Station

ISRO, Indian Space Research Organisation

LSTM, Land Surface Temperature Monitoring

MOBY, Marine Optical Buoy

MODIS, MODerate resolution Imaging Spectroradiometer

MODTRAN, MODerate resolution atmospheric TRANsmission

MSI, Multi-Spectral Instrument

MTF, modulation transfer function

NSO, near-simultaneous nadir observations

OCI, Ocean Color Instrument (of PACE)

OLI, Operational Land Imager

OOB, out-of-band

OSSE, Observing System Simulation Experiments

PACE, Phytoplankton Aerosols Clouds and ocean Ecology

PICS, pseudo invariant calibration sites

PRISMA, PRecursores IperSpettrale della Missione Applicativa (Hyperspectral Precursor of the Application Mission)

PROBA, Project for On-Board Autonomy, (ESA technology demonstration missions)

PTFE, Polytetrafluoroethylene

QVD, Quartz Volume Diffuser

RADCALNET, Radiometric Calibration Network

RSR, relative spectral response

SATM, Science and Applications Traceability Matrix

SBG, Surface Biology and Geology

SDSM, Solar Diffuser Stability Monitors

SHALOM, Space-borne Hyperspectral Applicative Land and Ocean Mission

SI, International System of Units

SNO, simultaneous nadir observation

SSO, Sun-synchronous orbit

SURFRAD, Surface Radiation Budget Network

SVC, system vicarious calibration

TIR, thermal infrared

TOA, top-of-atmosphere

TRISHNA, Thermal infraRed Imaging Satellite for High-resolution Natural resource Assessment

TSIS, Total Solar Irradiance Sensor (US NASA)

USGS, US Geological Survey

UMBC, University of Maryland, Baltimore County

VIIRS, Visible Infrared Imaging Radiometer Suite

VSWIR, visible-to-shortwave infrared

WATERHYPERNET, federated network of automated hyperspectral radiometers on zenith- and azimuth- pointing systems deployed on fixed structures, providing water reflectance data for satellite validation

WGCV, Working Group on Calibration and Validation of CEOS

